N93-30875

AN OVERVIEW OF THE CRASH DYNAMICS FAILURE BEHAVIOR OF METAL AND COMPOSITE AIRCRAFT STRUCTURES

Huey D. Carden
NASA Langley Research Center
Hampton, VA

Richard L. Boitnott
U.S. Army Aerostructures Directorate
NASA Langley Research Center
Hampton, VA

Edwin L. Fasanella, and Lisa E. Jones
Lockheed Engineering and Sciences Company
Hampton, VA

SUMMARY

An overview of the failure behavior results is presented from some of the crash dynamics research conducted with concepts of aircraft elements and substructure not necessarily designed or optimized for energy absorption or crash loading considerations. To achieve desired new designs which incorporate improved energy absorption capabilities often requires an understanding of how more conventional designs behave under crash type loadings. Experimental and analytical data are presented which indicate some general trends in the failure behavior of a class of composite structures which include fuselage panels, fuselage sections, individual fuselage frames, skeleton subfloors with stringers and floor beams without skin covering, and subfloors with skin added to the frame-stringer structure. Although the behavior is complex, a strong similarity in the static/dynamic failure behavior among these structures is illustrated through photographs of the experimental results and through analytical data of generic composite structural models. It is believed that the thread of similarity in behavior is telling the designer and dynamist a great deal about what to expect in the crash behavior of these structures and can guide designs for improving the energy absorption and crash behavior of such structures.

INTRODUCTION

The NASA Langley Research Center has been involved in crash dynamics research for several years, dating to the early 1970's. For about 10 years the emphasis of the research was on metal aircraft structures during the General Aviation Crash Dynamics Program (References 1 to 13) and the Controlled Impact Demonstration (CID) Program, a transport aircraft program which culminated in the controlled crash test of a Boeing 720 aircraft in 1984 (References 14 to 16). Subsequent to the transport work, the emphasis has been on composite structures with efforts directed at developing a data base for understanding the behavior, responses, failure mechanisms, and general loads associated with the composite material systems under crash type loadings (See figure 1). Considerable research has been conducted into determining the energy absorption characteristics (References 17 to 20) which indicated that composites can absorb as much if not considerably more energy than comparable aluminum structures. Because of the brittle nature of the composites, attention must be given to proper geometry and designs which will take advantage of their good energy absorbing properties while at the same time providing desired structural integrity when the composites are fabricated into aircraft structural elements and substructures. To achieve the desired new designs often requires an understanding of how more conventional designs behave under crash loadings.

The purpose of this paper is to present an overview of data on the failure behavior from research conducted with concepts of aircraft elements and substructure not necessarily designed or optimized for energy absorption or crash loading considerations. Experimental and analytical data are presented which indicate some general trends in the failure behavior of a class of composite structures which include fuselage panels, fuselage sections, individual fuselage frames, skeleton subfloors with stringers and floor beams but without skin covering, and subfloors with skin added to the frame-stringer arrangement. Although the behavior is complex, a strong similarity in the static and dynamic failure behavior among these structures is illustrated through photographs of the experimental results and through analytical data of generic composite structural models. It is believed that the thread of similarity in behavior is telling the designer and dynamist a great deal about what to expect in the crash behavior of these structures and can guide designs for improving the energy absorption and crash behavior of such structures.

IMPACT DYNAMICS RESEARCH FACILITY

The information presented in this report was generated and published during the transport and composite aircraft components phases of the impact dynamics research programs at NASA Langley Research Center. The research reported herein (with one exception) was conducted by personnel at the Langley Impact Dynamics Research Facility (shown in figure 2) and with other testing equipment associated with the installation. The facility is the former Lunar Landing Facility used to train astronauts for moon landings. The facility is 230 feet high and 400 feet long. Three sets of legs on the sides and two on the east end support the upper levels of the gantry. Access to the top levels is provided through an elevator. In the early 1970's, the structure was converted for crash testing of full-scale general aviation aircraft. Reference 21 provides complete details of the facility and test techniques for full-scale aircraft testing. Figure 3 is a photograph of a 70 foot high Vertical Drop Test Apparatus used for full-scale aircraft section, components, and/or seat testing. Static testing machines, and other apparatus are also added capabilities at the facility for metal and composite aircraft structural testing.

ANALYSIS TOOLS

To gain understanding of fundamental phenomena and the physics of behavior, the experimental research with structures under crash loadings is generally accompanied by analytical prediction or correlation studies whenever feasible. Thus, various finite element codes which have capabilities for handling dynamic, large displacement, nonlinear response problems of metal and composite structures are used as tools in the research efforts.

DYCAST Computer Code

The analytical results presented in this overview were generated with a nonlinear finite element computer code called DYCAST (DYnamic Crash Analysis of STructures (Reference 22) developed by Grumman Aerospace Corporation with principal support from NASA and FAA. The basic element library consists of (1) stringers or rod elements with axial stiffness only; (2) three-dimensional beam elements with 12 fixed cross-sectional shapes typical of aircraft structures with axial, two shear, torsional, and two bending stiffnesses; (3) isotropic and orthotropic membrane skin triangles with membrane stiffnesses; (4) isotropic plate bending triangles with membrane and out-of-plane bending stiffnesses; and (5) nonlinear translational or rotational spring elements that provide stiffness with user-specified force-displacement or moment-rotation tables (piece-wise linear). The spring element can be either elastic or dissipative. The springs are useful to model crush behavior of components for which data are available and/or whose behavior may be too complex or time consuming to model otherwise. A contractual effort is underway to add curved composite beams, composite plate, and curved shell elements to the DYCAST element library.

TEST SPECIMENS AND DESCRIPTION

Full-Scale Metal Aircraft Structures

NASA Langley Research Center has conducted several tests of metal aircraft sections to support transport research efforts. Selected data on the crash behavior of full-scale metal transport category aircraft sections (References 23 and 24) are included in the present paper to demonstrate what appears to be important similarities in behavior noted not only with the metal fuselage structures but also in the composite structures discussed herein.

Two 12-foot long fuselage sections cut from an out-of-service Boeing 707 transport aircraft were drop tested to measure structural, seat and occupant responses to vertical crash loads and to provide data for nonlinear finite element modeling. One section was from a location forward of the aircraft wings and one was from aft of the wing location. Figure 4 presents a photograph of one of the sections suspended in the Vertical Drop Test Apparatus at the Impact Dynamics Research Facility. The sections were loaded with seats, anthropomorphic dummies, data acquisition system pallet, power pallet, cameras, and batteries to test not only structure, seat, and occupant responses but also to test the pallet equipment to be used in the full-scale transport crash conducted later. The reader should refer to the particular reports for more complete descriptions of the test articles since such information is not repeated in this report.

Composite Structures

Composite Fuselage Panel.-As part of the Aircraft Energy Efficiency (ACEE) Program, static and dynamic behavior of a lower fuselage composite structure was evaluated (reference 25). Development tests were performed on the composite structures to verify that the composite structure, designed to the same operating load as the metal design, could have at least the same energy absorption capability as aluminum structure. A photograph of the composite fuselage panel in the static testing machine (at Lockheed-California Company) is shown in figure 5 . Load-displacement and failure behavior determined for the corrugated frame/skin test panel are included herein for comparison with other composite structures. The frame/skin specimen had a 117.5 inch radius (to outside skin), was 60 inches long by 30 inches wide and had two corrugated frames on 20 inch spacing. Fabrication techniques and more complete details of the frame/skin panel are given in reference 25.

Single Composite Frames.- Various cross-sectional shapes for fuselage frames are used in metal aircraft and are often proposed for composite aircraft structures. Figure 6 presents sketches and photographs illustrating four of the more common geometries, I-, J-, C- and Z-cross sectional shapes of which several circular frames were fabricated for testing to add to the composite structures data base. To add out-of-plane stability to the frame concepts (with the exception of the Z-section frames), 3 1/2 inch wide skin material was added which enhanced the ease of testing of both symmetric and other antisymmetric sections. The skin, a $[\pm 45/0/90]_{2s}$ lay-up sixteen ply (.08 inches) thick, was cocured with the 6 foot diameter frames. The frames were constructed in two different heights, 1 1/4 inches high and 3/4 inches high, to investigate the effect of frame height on behavior and responses.

One of the first geometries to be studied under static and dynamic loadings was the Z-cross section. Figure 6(b) is a photograph of Z-cross section fuselage frames used in the initial studies of the behavior of composite structural elements under impact loads. Figure 7 shows a Z-frame suspended in the drop apparatus prior to testing. The apparatus was constructed with guide rails, a rear metal backstop, and a front Plexiglas sheet. During free-fall the specimen was guided, and the front and rear backstops prevented appreciable (but not all) out-of-plane bending or twisting during impact and allowed photographs/motion picture coverage through the front Plexiglas plate . The six-foot diameter frames were constructed of 280-5HA/3502, a five harness satin weave graphite fabric composite material. The height of the frame was 3 inches with a total width of 2.25 inches and was about 0.08 inches thick. Lay-up of the frames was quasi-isotropic. Initial tests were with 360° frames made from four 90°segments joined with splice plates as shown

in figure 6(b). Additional tests were conducted with half frames since the top half of the complete frames were undamaged in the tests.

The approach of studying simple structural elements and then moving to combinations of these elements into more complex substructures has been taken in the development of a data base on the dynamic response and behavior of composite aircraft structures. The approach parallels the one used during the general aviation and transport aircraft programs. Consequently, three composite subfloor structures were fabricated following the initial investigation of the Z-frames discussed above.

Subfloor Structures.- Figure 8 is a photograph of the skeleton and skinned subfloor specimens constructed with three of the single Z-section frames similar to those that were studied earlier. Pultruded J-stringers attached the three frames through metal clips and secondary bonding methods. Aluminum floor beams tied the top diameter of the frames together to form the lower half of the subfloor. Notches in the frames allowed the stringers to pass through the frames. Two subfloors without skin (called skeleton subfloors) were fabricated. A third specimen (called skinned subfloor) had a ±45 lay-up skin bonded and riveted to the frames to form the lower fuselage type structure.

RESULTS AND DISCUSSION

Figures 9 to 20 present results from the studies of full-scale aircraft structures, composite fuselage frames, and subfloors under static and/or dynamic loadings. Analytical results are also included which illustrate crash related behavior of some of the structures. Photographs are included which emphasize the failure behavior of the composite and metal aircraft components and show a strong similarity in their behavior. The behavior is thought to be an important aspect which must be considered in the design of new structures for improving the energy absorption and crash behavior of this type components and structural elements.

Full-Scale Metal Aircraft Structures

Experimental and analytical results from studies with full-scale transport category aircraft sections (References 23 and 24) are presented in figure 9.

Dynamic tests.- Structural damage and behavior of the transport aircraft structures resulting from the 20 ft/s drop tests is shown in figure 9(a) and (b). The damage to the transport sections was confined to the lower fuselage below the floor level. Under the vertical impact of 20 ft/s, all seven of the frames ruptured near the bottom impact point. Plastic hinges formed in each frame along both sides of the fuselage at about 50° up the circumference from the bottom contact point (See figure 9(c)). The upward movement of the lower fuselage was approximately 22-23 inches at the forward end and 18-19 inches at the rear for the section taken from forward of the wing location (figure 9(a)) whereas in the section from aft of the wing location (figure 9(b)), the crushing was about 14 inches forward and 18 inches in the rear. Although the aircraft structures are metal and the failures discussed above involve plastic deformations with some tearing of the metal rather than brittle fractures, the general observed failure pattern and locations for the transport fuselage sections will be shown to be quite similar to the results of the composite frames and subfloors discussed later.

Analytical studies.- A DYCAST model of the section (from forward of the wing location) was constructed with sufficient detail to model the floor, two seats with lumped mass occupants, and the fuselage structure to determine if such a model could predict the response of the complete section with fidelity. The geometry of the finite element model is shown in figure 10. Stiff ground springs simulated the concrete impact surface. Each frame of the fuselage below the floor was modeled with eight beam elements and floor and seat rails were also appropriate beam elements. Fuselage structure above the floor (not expected to fail) was modeled in less detail.

The predicted deformation pattern of the two frame model is shown in figure 11. As may be noted, the overall impression from the analytical model deformation pattern is quite similar to the visual behavior seen in the experiment shown in figure 9. The full section behavior was basically contained in the two frame model.

In the following sections the composite impact dynamics studies have taken the building block approach of utilizing a sequence of testing and analysis which begins with 'simpler' elements and moves to more 'complicated' components or substructures. As mentioned earlier, this approach was used in the General Aviation and Transport programs although the GA data base was being concurrently developed through full-scale testing. Eventually it is desired to add to the program the full-scale tests using currently available composite aircraft specimens and/or other full-scale structures that are designed and constructed for that purpose.

Composite Fuselage Panel Study

Static load-displacement data for the corrugated frame/skin specimen from the ACEE program and the failure behavior are shown in figure 12. Figure 12(a) indicates that the load increased linearly to failure whereupon the load dropped substantially as a result of fracturing of the corrugated frames at locations (0° and 6.2°) near the center (loading region) of the panel. Additionally, some delamination of the frame caps occurred during the loading. Once the panel was removed from the test apparatus, the snap-through condition of the skin was reversed as may be noted in the figure 12(b). The fractures of the corrugated frame and some delamination of the frame caps, mentioned above, are the only visible damage to the structure.

Composite Single Frame Studies

Static tests.- Figure 13 presents static results from tests of single composite Z-frames discussed in reference 26. A photograph of the static test apparatus in figure 13(a) shows that the splice plate was at the load point. The frame failed just outside the doubler splice plate area by a complete fracture across the Z-section. Load-deflection data and the location of failures of the frame are shown in figure 13(b). The load-deflection data show a saw-toothed behavior beginning with the essentially linear behavior of the frame up to initial failure with subsequent loading of the frame after failure being at a new, reduced stiffness for the damaged frame. Photographic data in figure 13(c) show that the initial failure was induced by a local buckling of the frame which occurred at about 18° from the bottom loading point outside the splice plate area. Second and third fractures occurred up the side at about 54° and 58° under continued loading as may be noted in the sketch at the right of figure 13(b). The sequence of events was local buckling near the splice plate induced out of plane deformations which led to a fracture of the section; the ends then remained in contact (jammed together under the compressive loads in the frame), the initial point of fracture moved vertically, essentially in a guided manner until two additional fractures occurred farther up the frame.

Static analytical studies.- To demonstrate analytically the apparent behavior of the frames under load (exclusive of the local buckling which actually initiated the failure in the static case), a DYCAST finite element model was constructed. For ease of analysis, an I-section was modeled from the specimens described in the "Single Composite Frame" section. The frame was loaded at the top and a simulated ground plane (ground contact springs) resisted the vertical movement of the frame during load application. Boundary conditions were imposed at the bottom node of the model to account for the symmetrical situation thus only half the frame had to be modeled. The top node was constrained to allow only vertical displacement thus simulating the effect of a very stiff floor across the frame diameter. The static load was slowly increased until an input failure strain for the material (0.0086) was exceeded at the point of loading and failure was indicated. The curve labeled case I, *unbroken frame,* in figure 14(a) is the load-deflection plot for this case.

An examination of the normalized distribution of the bending moment on the frame shown in figure 14(b) provides insight and a better understanding of the failure/behavior. Maximum moments are indicated (just prior to failure) to be at the 0° location and between 50°-60° from the bottom contact area. The locations correlate well with the failure locations in the experiment with the Z-frame.

A second DYCAST model, case II, was also run wherein the bottom point of the frame was modeled with two short skin segments to represent the different structural condition following the initial failure of the frame. This condition will be discussed further, relative to the composite subfloor test with the skinned subfloor specimen. The curve in figure 14(a) labeled case II, *broken frame,* is the load-deflection response for this frame-loading case. Initially, the frame load increases to the point of failure at the bottom of the frame. After the frame fractures, the structure (boundary) changes to one considerably weakened--down to the bending stiffness of the skin alone at that location. The load therefore drops to the lower curve which represents the stiffness of the section with the weakened boundary on the bottom end of the frame, as indicated by the dashed vertical line between the case I curve and the case II curve. The load continues to increase again along the *broken frame* case until a failure at some other locations on the frame circumference occurs, thus repeating the cycle.

Figure 14(c) presents the normalized bending moment distribution on the broken frame. As may be noted, the distribution is quite similar to the initial model results in figure 14(b). The failure location is at the maximum bending moment location predicted to be about 45° which is somewhat lower than the same location shown in the initial model of the unbroken frame. The agreement between the two models, however, is still considered good. The effect of diameter on the moment distribution of the frame was assessed with a model having a 75 inch diameter (twice the initial diameter). The distribution was identical to the smaller diameter results; however, the loads producing the moments differed between the two models (as expected).

A comparison of the analytical cases (figure 14(a)) with the actual static load-deflection of the Z-section (figure 13(b)) indicates very similar load-deflection behavior patterns as discussed above. Although the Z-frame had no skin, if the ends jam together (as they did in several cases), the boundary is effectively between the skin stiffened case and a guided boundary. Thus, the predicted failure location in the simple beam-frame model at about 50° (See figure 14(b)) agrees well with the 54° and 58° failure locations in the experiment with the Z-section frame.

Without a priori knowledge of the manner of the failure noted and discussed above, the initial formulation of a finite element model would unlikely incorporate the necessary failure mechanism/behavior for the frames. However, knowing the pattern of behavior can enable the analysts to formulate adequate finite element models to predict dynamic responses including the failure/loads. Additionally, such information is important to designers of new structures to be able to design for impact loads on such structural elements of an aircraft fuselage.

Dynamic tests.- Figure 15 presents results from the dynamic studies of the response of composite frames (Reference 27). As noted in figure 15(a) or (b), the splice plates joining the segments of the frame are ±45° up the circumference from the point of impact. As shown in figure 15(b) complete failures (fractures) of the Z-section frames occurred at the bottom and approximately ±60° from the bottom. Potentially, it appears that the presence of the splice plates may have influenced the locations by moving the top failure points up a few degrees to about the ±60° locations.

Composite Subfloor Studies

For the three composite subfloor specimens used for impact studies, two static and two dynamic tests were conducted on the subfloors. With the skeleton subfloor, both a static and a dynamic test to destruction was conducted. With the skinned subfloor, a nondestructive static test followed by a dynamic test to failure was conducted.

Static tests.- Figure 16 presents experimental results (Reference 28) of the skeleton subfloor specimen following a static test. As noted in figure 16(a) and (b), failures on the three Z-section frames occurred at 13 discrete locations. Unlike the unnotched single Z-frame, the failures in this specimen occurred at notches (which served as stress risers) in the frame through which the stringer passed. However, as shown in figure 16(b) the failures were still near the point of load application (approximately 11°) and at other circumferential

locations of approximately 45-68°. In the absence of skin material, twisting and bending out-of-plane occurred with the frames. The stringers had minimal effect on the subfloor response with the exception of maintaining the lateral spacing of the three Z-frames.

Dynamic tests.- Figure 17 shows the skeleton subfloor after an impact test onto a concrete surface at 20 feet per second. In the dynamic test of the skeleton subfloor, fractures were produced at notches in the frames (Figure 17(a)). The locations, shown in figure 17(b), were also near the point of impact (about 11° because of the splice plate) and at two other locations up the circumference of the frames (±45° and ±78°) and involve all three frames for a total of 15 fractures. The impact energy exceeded the energy absorbed by the local fractures and the floor bottomed out in the impact. Figure 17(c) is a normalized strain distribution measured on the first (end) frame during the dynamic test just before first failure. A comparison of the distribution to the moment distribution of Figure 14(b) and (c) shows essentially identical shape between the single frame and skeleton frame distributions. Maximums at 0° and at approximately ±50° to 55° agree well with the analytically predicted locations on the frame.

Figure 18 presents impact results for the subfloor with skin after an impact of 20 feet per second. Figure 18(a) is the subfloor specimen after the test. Points of failure of the frames in this specimen are indicated in figure 18(b). Again the points of failure are at/near the impact point (within 12°) and on the circumference at about ±56° up both sides of the frame on the middle and back frame and 11°, 22.5° and 45° on the front frame. It was observed that the subfloor impacted first on the front area which possibly explains the 11° and 22.5° fractures being different from the other locations. Again all three frames were involved in the failures. Some delamination of the frames from the skin was evident but the skin remained intact. Figure 18(c) is a normalized strain distribution (just prior to first failure) measured on the first (end) frame during the dynamic test. A comparison of the distribution to the moment distribution of Figure 14(b) and (c) and the strain distribution in Figure 18(c) shows essentially identical shape as the single frame and skeleton frame distributions. As was the case for the skeleton subfloor maximums at 0° and at approximately ±50° to 55° agree well with the analytically predicted locations on the frame.

As mentioned previously in the frame studies, once the frames fail at or near the point of impact the broken ends of the frame often jammed together and moved upward in a guided manner. In the subfloor structure, the frames may still fail completely across the section, but the skin remains intact and serves as a much less stiff boundary condition for the broken frames as the deflection increases. Little energy is involved in snapping the skin through as the load increases on the structure (See reference 29 on snap-through of composite arches). In this manner, the structural stiffness of the frame/skin before fracture changes to the skin only at the location of frame fracture. The analytical models discussed under the static frame response/behavior simulated this type of behavior.

Analytical studies.-The contribution of the skin to the stiffness of the section with the antisymmetric frames is illustrated in figure 19. Static load-deflection data for the unskinned subfloor and the skinned subfloor along with the DYCAST predictions are shown in the figure. It can be noted that the subfloor stiffness (with skin) is approximately three times the stiffness of the skeleton subfloor, thus the skin's contribution to the structure is to maintain in-plane deflections of the non-symmetrical Z-section and prevent any substantial twisting of the frames. Out-of-plane bending and twist were allowed in the skeleton subfloor predictions. As a further note of interest, if for the skeleton subfloor, load in the load-deflection results (with three frames) is reduced by a factor of three, good correlation with single frame data is evident.

General Observations

The response behavior determined during the studies of full-scale aircraft sections, fuselage panels, fuselage frames, and subfloors are summarized in figure 20. Figure 20(a) shows normalized moment distribution on a representative frame of the various specimens and Figure 20(b) shows the failure locations which were noted from static or dynamic tests. The visual impression is quite striking among the various specimens. It is suggested that from the results of simpler frames to the more complex subfloors and full-scale sections, a strong similarity is evident in the failure behavior of the structures. The structures share in

common the generally circular or cylindrical shape, the normal loading situations, and what appears to be a similar pattern of failure behavior. Analytical models of frame structures under vertical loads have moment distributions which have maximums at the point of loading and at approximately ±45° to 50° (depending on boundary conditions) around the circumference from the ground contact point. Failures of the structures were noted at these same locations. Such observations can help dynamists gain a better understanding of what to expect from such structures in crash-loading situations, can guide designers of new structures to better account for the vertical crash loads, and allow better energy absorption to be included in the new designs. Additionally, the observations can help analysts better model the aircraft structures for predicting the failure responses and behavior under crash situations. The latter task is a difficult and challenging one, not only for composite structures but for metal structures as well. Studies are currently underway to improve the analysis capabilities of code and to add composite elements to finite element libraries such as the DYCAST program. In addition, new analysis approaches are being explored through grants to universities as an extension of NASA Langley Research Center's efforts.

CONCLUDING REMARKS AND OBSERVATIONS

Some unique failure behavior results from the research with composite full-scale aircraft sections, composite structural elements, and subfloors have been presented. Some observations on the failure behavior of these structures have been made and discussed and analytical results have been included to help explain some of the behavior noted.

From the observations made in the overview the following conclusions are made:

(1) Starting with simple representative structural elements and moving to more complex components can often provide better understanding of the complex local and global structural responses and behavior.

(2) Unique failure behavior patterns were found to be common among full-scale fuselage panels, aircraft sections, composite frames, and subfloors with and without skin.

(3) General locations of failures appear to occur at the same structural regions among the specimens as a result of similar geometry (cylindrical shape), similar loading (vertical), and similar moment distribution on the structures under vertical loads.

(4) Noted failures were located in the same regions as the maximums in the moment (strain) distribution on the structures.

(5) The shape of the distribution of the moment was independent of the size (diameter) of the frame/component. Loads, however, which produced the failures varied with the structural size.

Based upon the conclusions drawn from the various research efforts discussed in this paper, the following observations are also summarized:

(1) The general similarity of the failure behavior among the aircraft structures can

(a) assist the designer and dynamist to better anticipate how the structures probably will fail.

(b) provide guidance on how and where to incorporate and/or optimize better energy absorption into new aircraft structural designs.

(c) aid analysts to better model the structures for predicting failure/loads behavior under crash situations.

(2) To analytically predict, in a dynamic loading situation, such complex failure events and the loads which initiate the failures as noted in the composite structural elements and sub-components is a challenge.

(3) Composite curved beam, composite plate, and shell elements that are being developed and included in finite element code should improve the capability to analyze composite type structures.

REFERENCES

1. Alfaro-Bou, Emilio; and Vaughan, Victor L., Jr.: Light Airplane Crash Tests at Impact Velocities of 13 and 27 m/sec. NASA TP 1042, November 1977.

2. Castle, Claude B.; and Alfaro-Bou, Emilio: Light Airplane Crash Tests at Three Flight-Path Angles. NASA TP 1210, June 1978.

3. Hayduk, Robert J.: Comparative Analysis of PA-31-350 Chieftain (N44LV) Accident and NASA Crash Test Data. NASA TM 80102, October 1979.

4. Castle, Claude B.; and Alfaro-Bou, Emilio: Light Airplane Crash Tests at Three Roll Angles. NASA TP 1477, October 1979.

5. Vaughan, Victor L., Jr.; and Alfaro-Bou, Emilio: Light Airplane Crash Tests at Three Pitch Angles. NASA TP 1481, November 1979.

6. Vaughan, Victor L., Jr.; and Hayduk, Robert J.: Crash Tests of Four Identical High-Wing Single-Engine Airplanes. NASA TP 1699, August 1980.

7. Carden, Huey D.; and Hayduk, Robert J.: Aircraft Subfloor Response to Crash Loadings. SAE Paper 810614, April 1981.

8. Williams, M. Susan; and Fasanella, Edwin L.: Crash Tests of Four Low-Wing Twin-Engine Airplanes with Truss-Reinforced Fuselage Structure. NASA TP 2070, September 1982.

9. Carden, Huey D.: Correlation and Assessment of Structural Airplane Crash Data with Flight Parameters at Impact. NASA TP 2083, November 1982.

10. Carden, Huey D.: Impulse Analysis of Airplane Crash Data with Consideration Given to Human Tolerance. SAE Paper 830748, April 1983.

11. Castle, Claude B.; and Alfaro-Bou, Emilio: Crash Tests of Three Identical Low-Wing Single-Engine Airplanes. NASA TP 2190, September 1983.

12. Thomson, Robert G.; Carden, Huey D.; and Hayduk, Robert J.: Survey of NASA Research on Crash Dynamics. NASA TP 2298, April 1984.

13. Carden, Huey D.: Full-Scale Crash Test Evaluation of Two Load-Limiting Subfloors for General Aviation Airframes. NASA TP 2380, December 1984.

14. Hayduk, Robert J.(Editor): Full-Scale Transport Controlled Impact Demonstration. NASA CP 2395, April 1985.

15. Fasanella, Edwin L.; Widmayer, E.; and Robinson, M. P.: Structural Analysis of the Controlled Impact Demonstration of a Jet Transport Airplane. AIAA Paper 86-0939-CP, May 1986.

16. Fasanella, Edwin L.; Alfaro-Bou, Emilio; and Hayduk, Robert J.: Impact Data from a Transport Aircraft During a Controlled Impact Demonstration. NASA TP 2589, September 1986.

17. Farley, Gary L.: Energy Absorption of Composite Materials. NASA TM 84638, AVRADCOM TR-83-B-2, 1983.

18. Bannerman, D.C.; and Kindervater, C.M.: Crashworthiness Investigation of Composite Aircraft Subfloor Beam Sections. IB 435-84/3(1984), Deutsche Forschungs-und Versuchasanstalt fur Luft- und Raumfarht, February 1984.

19. Cronkhite, J.D.; Chung, Y.T.; and Bark, L.W.: Crashworthy Composite Structures. ASAAVSCOM TR-87-D10, U.S. Army, December 1987. (Available from DTIC as AD B121 522.)

20. Jones, Lisa E.; and Carden, Huey D.: Evaluation of Energy Absorption of New Concepts of Aircraft Composite Subfloor Intersections. NASA TP 2951, November 1989.

21. Vaughan, Victor L.; and Alfaro-Bou, Emilio: Impact Dynamics Research Facility for Full-Scale Aircraft Crash Testing. NASA TN D-8179, April 1976.

22. Pifko, A.B.; Winter, R.; and Ogilvie, P.L.: DYCAST - A Finite Element Program for the Crash Analysis of Structures. NASA CR 4040, January 1987.

23. Williams, M. Susan; and Hayduk, Robert J.: Vertical Drop Test of a Transport Fuselage Section Located Forward of the Wing. NASA TM 85679, August 1983.

24. Fasanella, Edwin, L.; and Alfaro-Bou, Emilio: Vertical Drop Test of a Transport Fuselage Section Located Aft of the Wing. NASA TM 89025, September 1986.

25. Jackson, A.C.; Balena, F.J.; LaBarge, W.L.; Pei, G.; Pitman, W.A.; and Wittlin, G.: Transport Composite Fuselage Technology--Impact Dynamics and Acoustic Transmission. NASA CR 4035, Contract NAS1-17698, December 1986.

26. Boitnott, Richard L.; and Kindervater, Cristof: Crashworthy Design of Helicopter Composite Airframe Structure. Fifteenth European Rotorcraft Forum, Amsterdam, Holland, Paper Nr; 93, September 1989.

27. Boitnott, Richard L.; Fasanella, Edwin L.; Calton, Lisa E.; and Carden, Huey D.: Impact Response of Composite Fuselage Frames. SAE Paper 871009, April 1987.

28. Boitnott, Richard L.; and Fasanella, Edwin L.: Impact Evaluation of Composite Floor Sections. SAE Paper 891018, General Aviation Aircraft Meeting and Exposition, Wichita, Kansas, April 1989.

29. Carper, Douglas M.; Hyer, Michael W.; and Johnson, Eric R.: Large Deformation Behavior of Long Shallow Cylindrical Composite Panels. Virginia Polytechnic Institute and State University, VPI-E-83-37, September 1983.

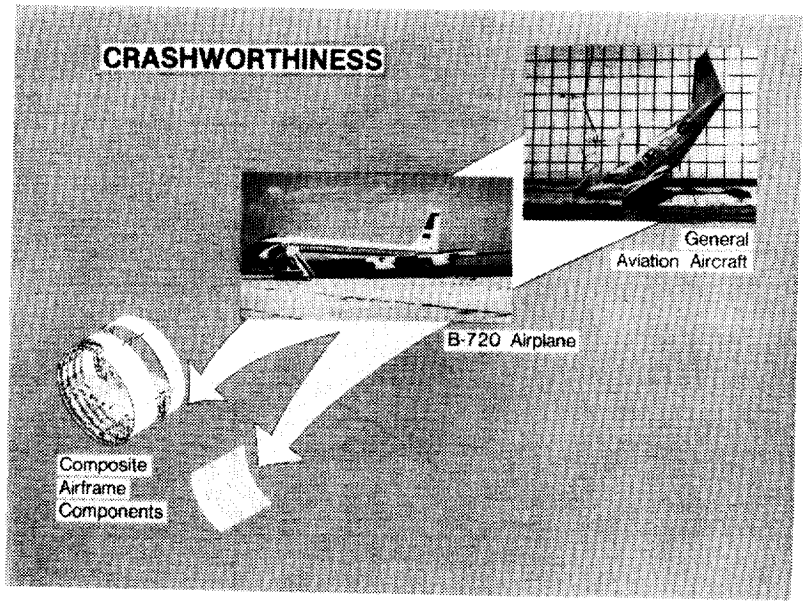

Figure 1.- Progression of research areas in crash dynamics at NASA Langley Research Center.

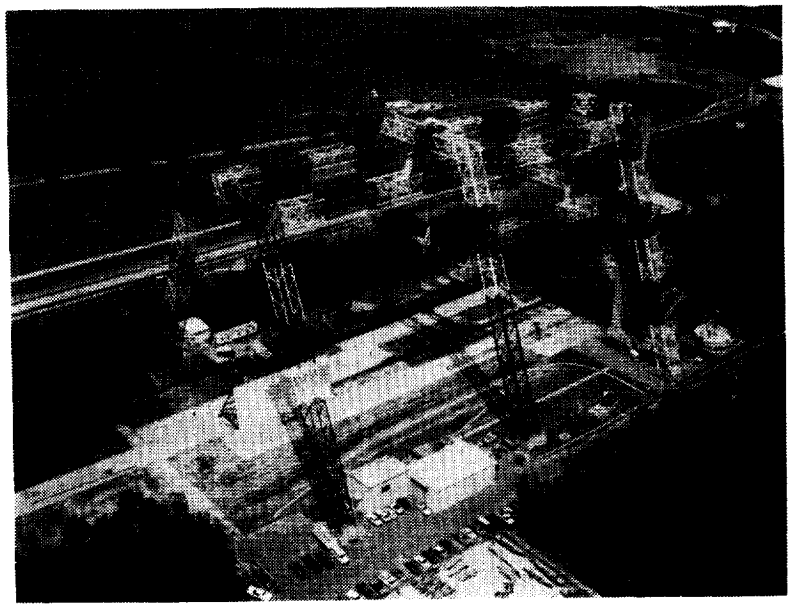

Figure 2. - Impact Dynamics Research Facility (IDRF) a NASA Langley Research Center.

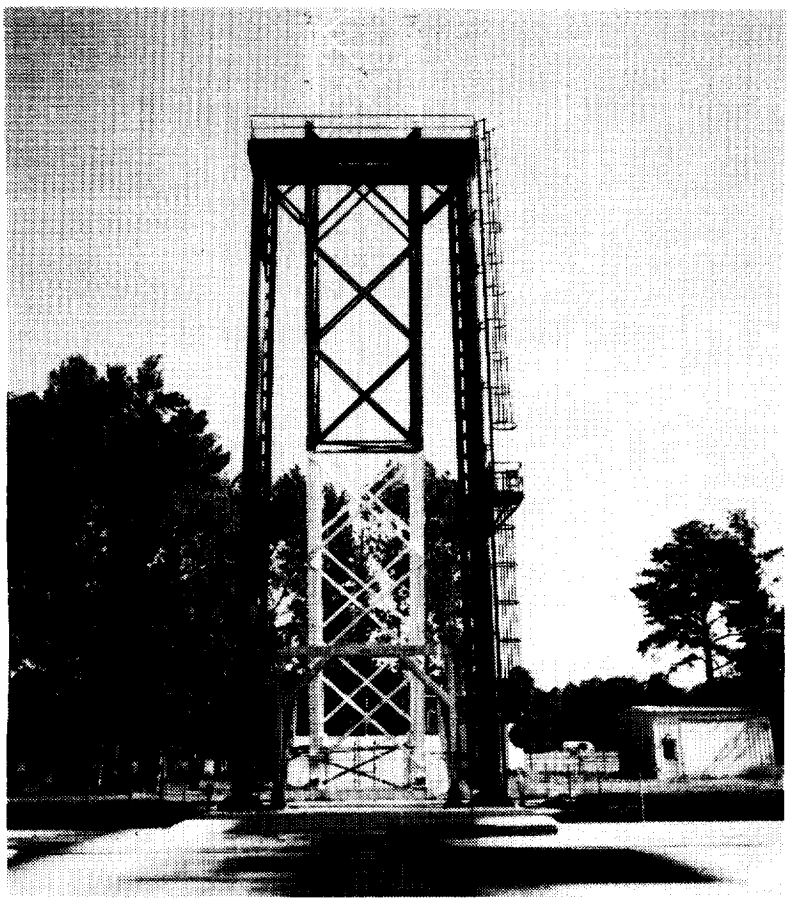

Figure 3. - 70 Foot Vertical Drop Test Apparatus.

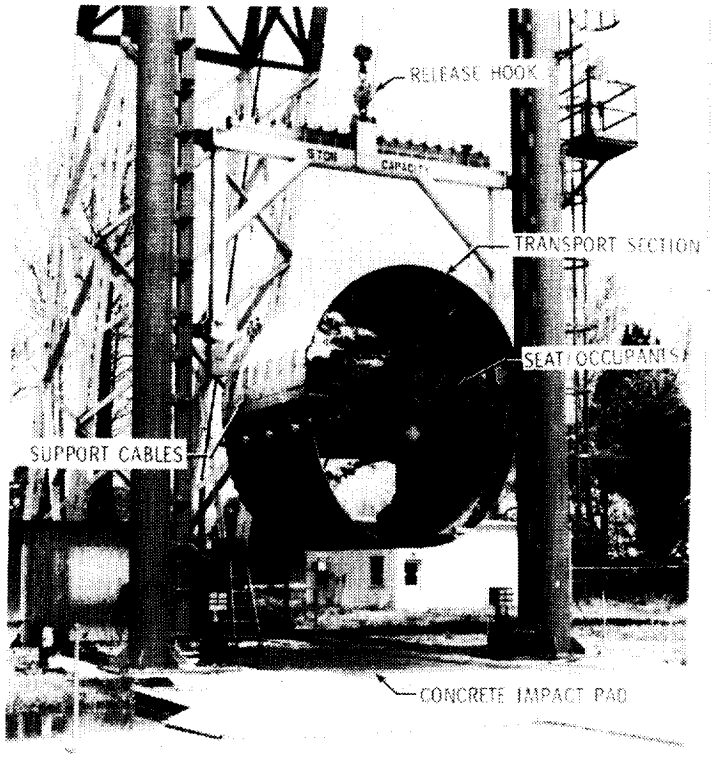

Figure 4. - Metal transport section suspended in Vertical Test Apparatus.

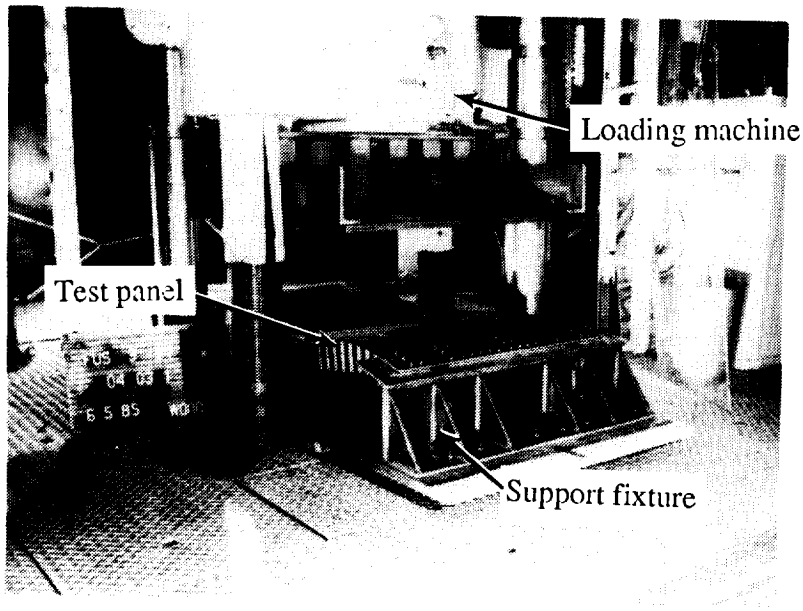

Figure 5.- Composite fuselage panel in static test machine. Panel from Aircraft Energy Efficieny (ACEE) Program. Photo courtesy of Lockheed-California Company.

ORIGINAL PAGE
BLACK AND WHITE PHOTOGRAPH

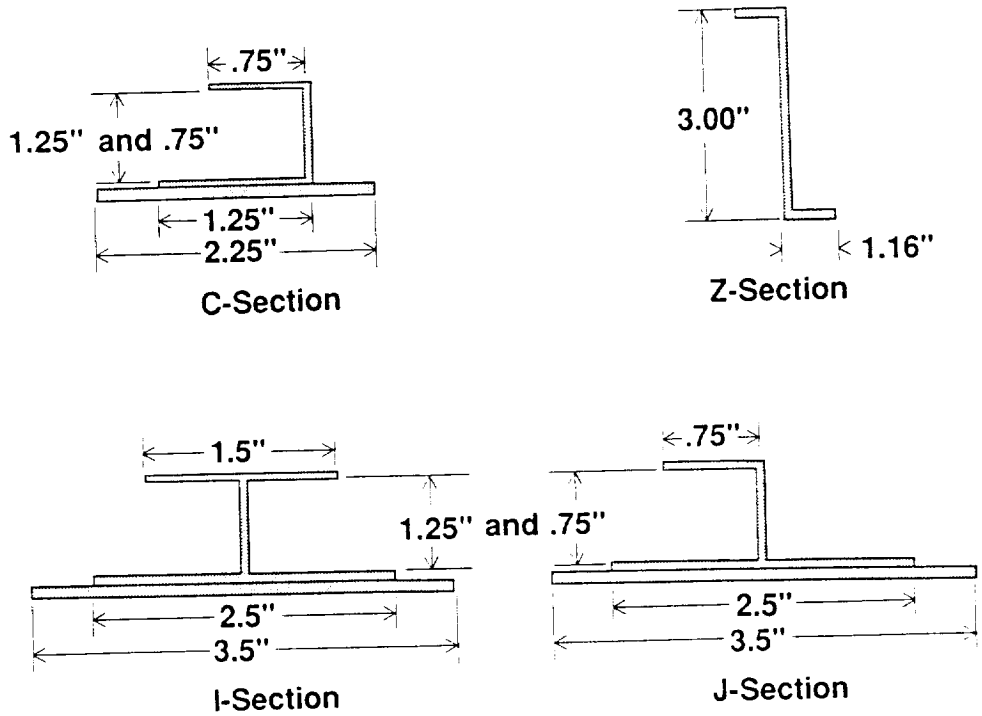

(a) Cross-sectional dimensions.

Figure 6.- Various cross-sectional shapes of composite fuselage frames.

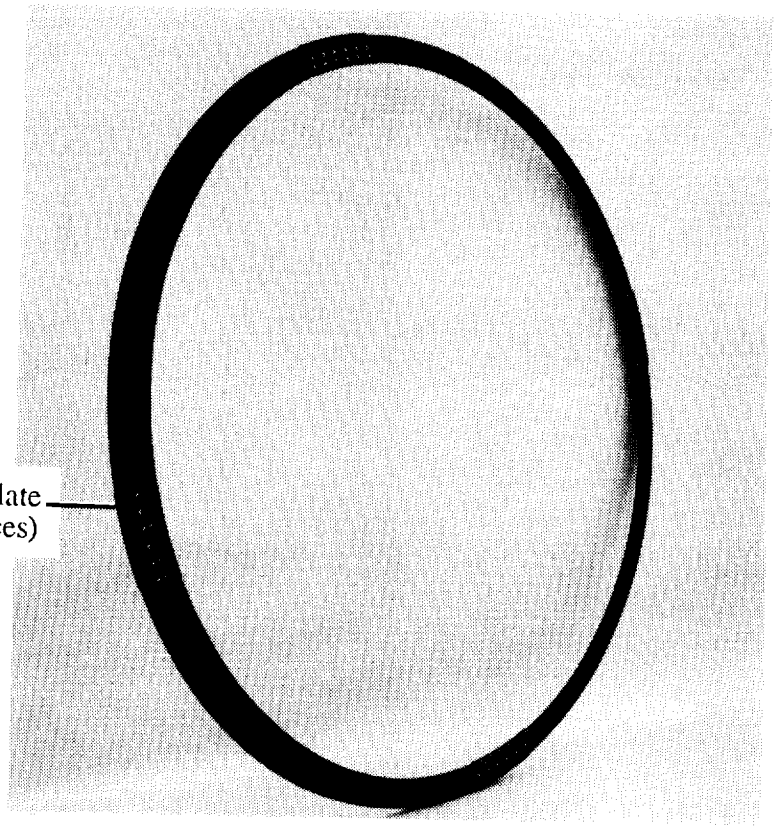

(b) Z-cross section fuselage frame.

Figure 6.- Concluded.

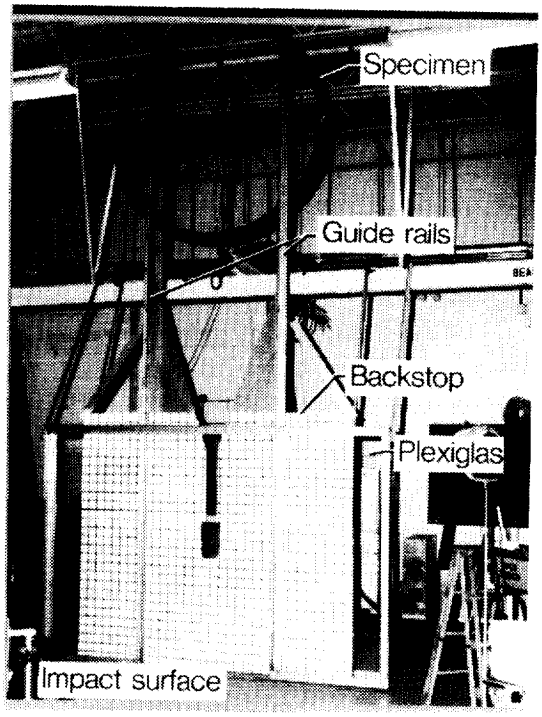

ORIGINAL PAGE
BLACK AND WHITE PHOTOGRAPH

Figure 7.- Composite Z-frame in drop apparatus.

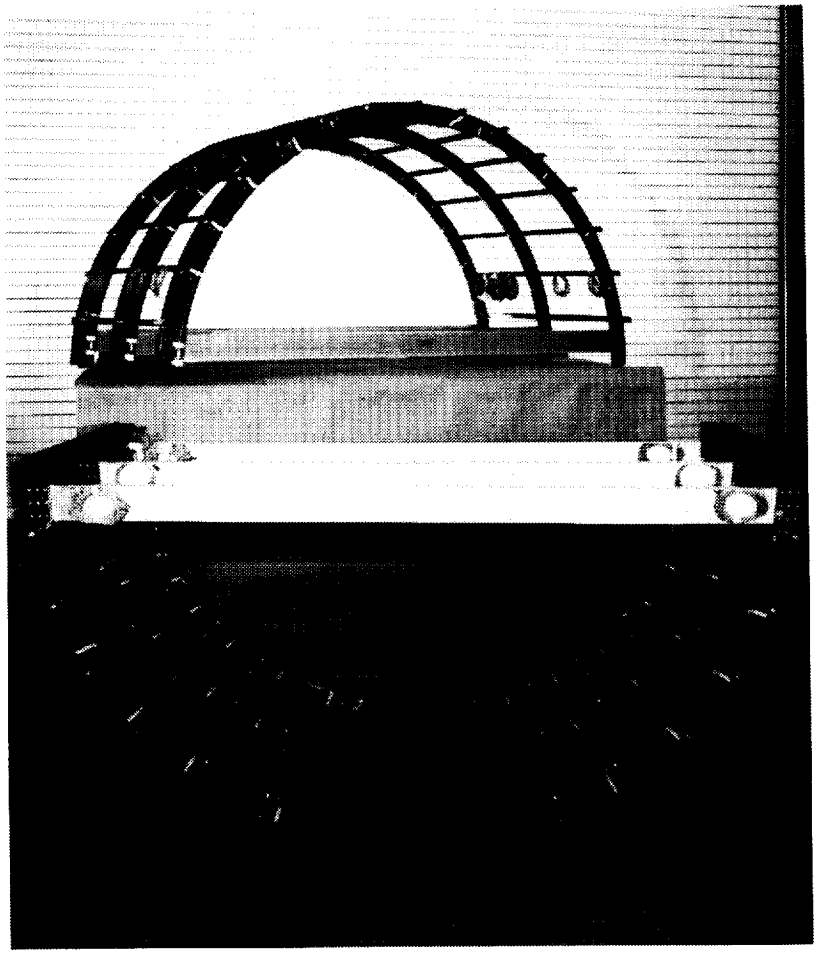

Figure 8.- Composite subfloor sections (skeleton/unskinned (top), skinned (bottom)).

ORIGINAL PAGE
BLACK AND WHITE PHOTOGRAPH

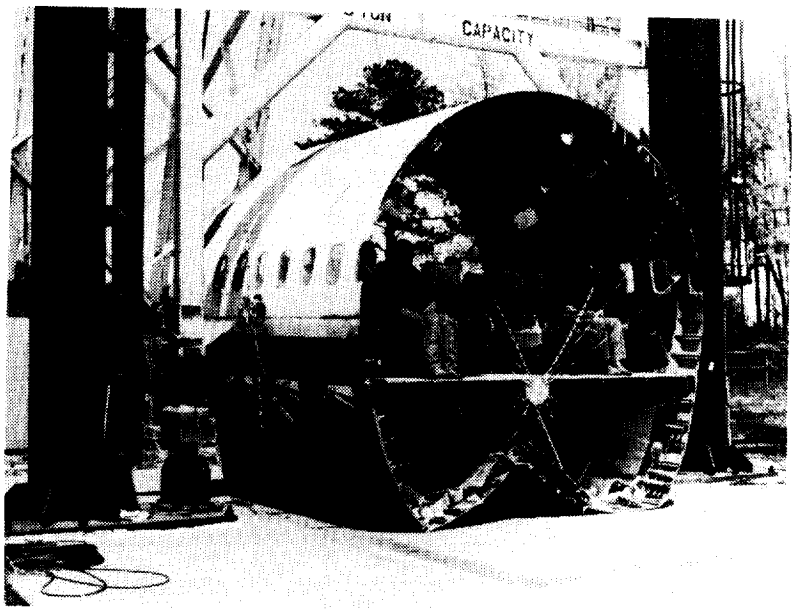

(a) Section from forward of wing.

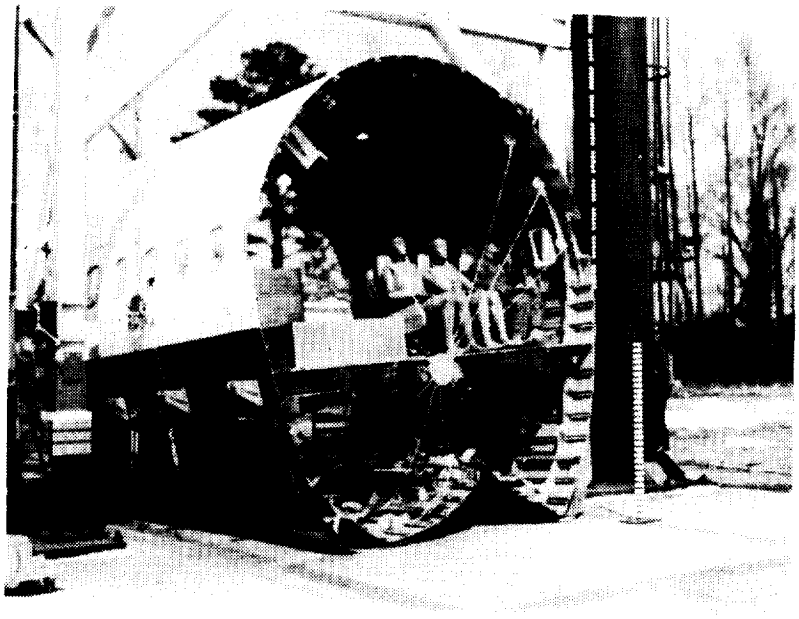

(b) Section from aft of wing.

Figure 9.- Structural damage to metal aircraft structures.

ORIGINAL PAGE
BLACK AND WHITE PHOTOGRAPH

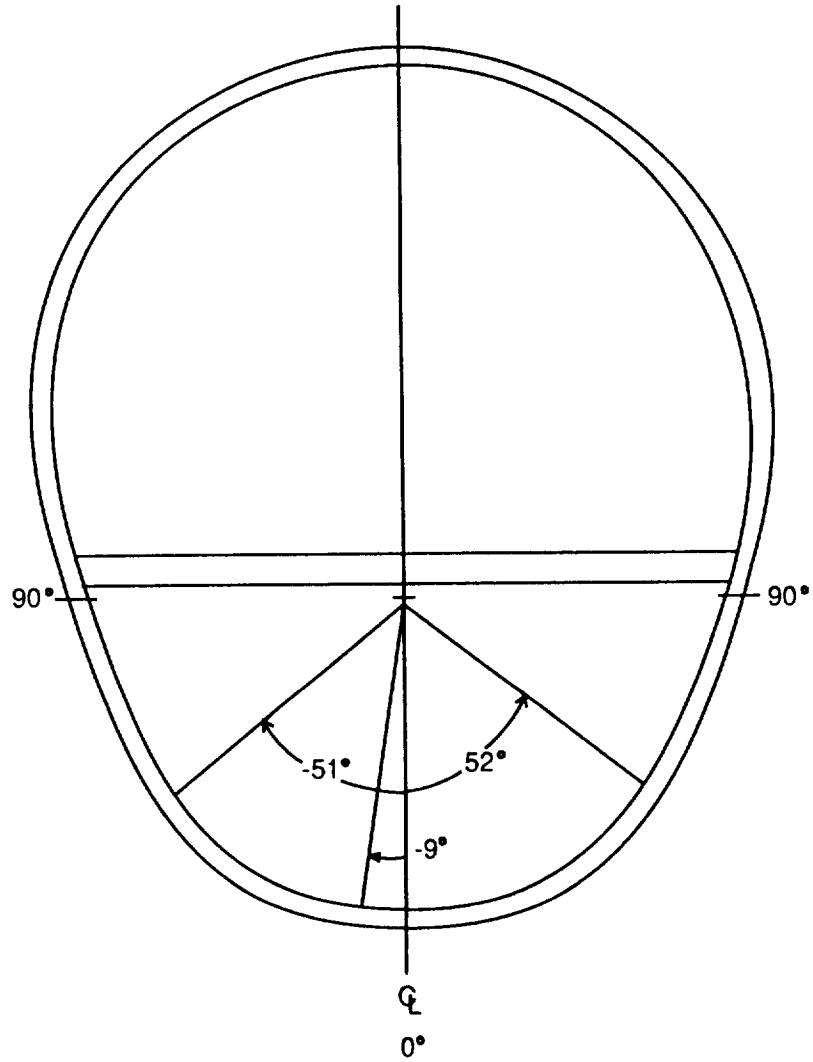

(c) Angular location of failures.

Figure 9.- Concluded.

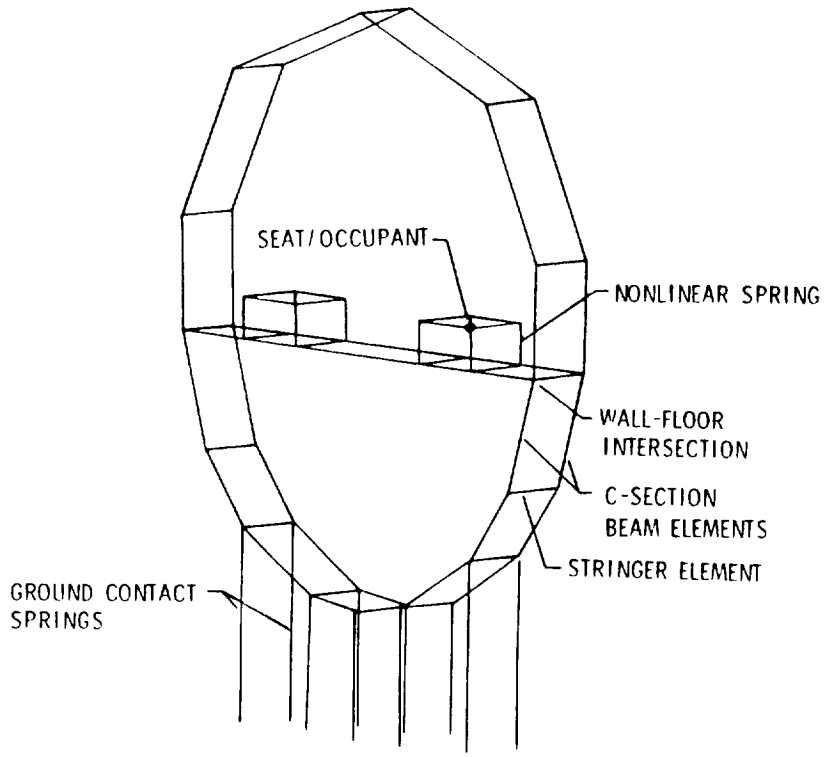

Figure 10.- Finite element two-frame model of metal transport section.

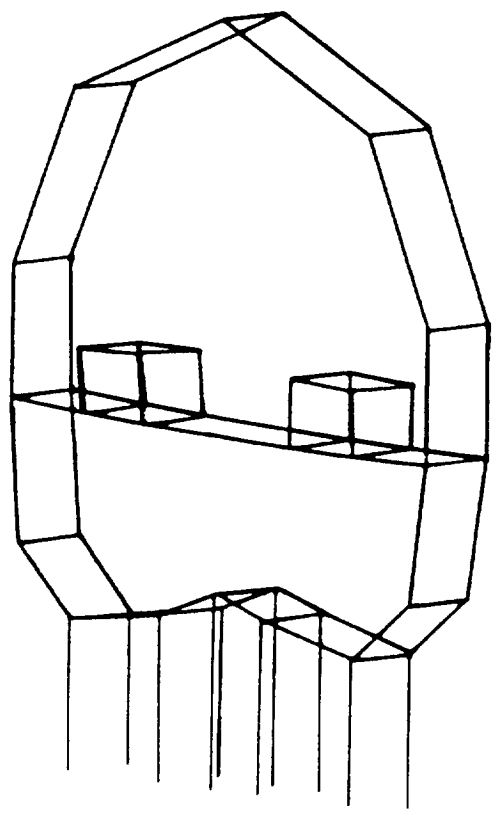

Figure 11.- Computer graphics showing analytical failure of metal transport section.

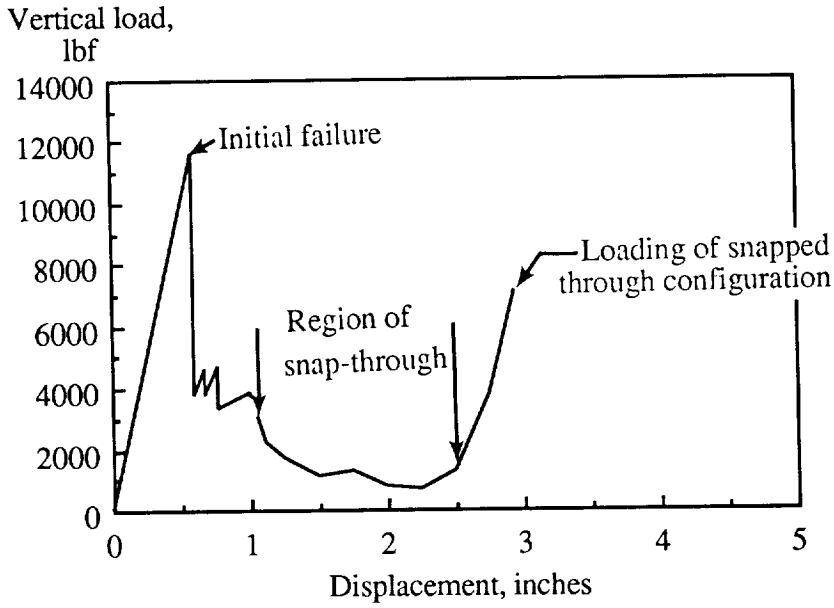

(a) Load-displacement.

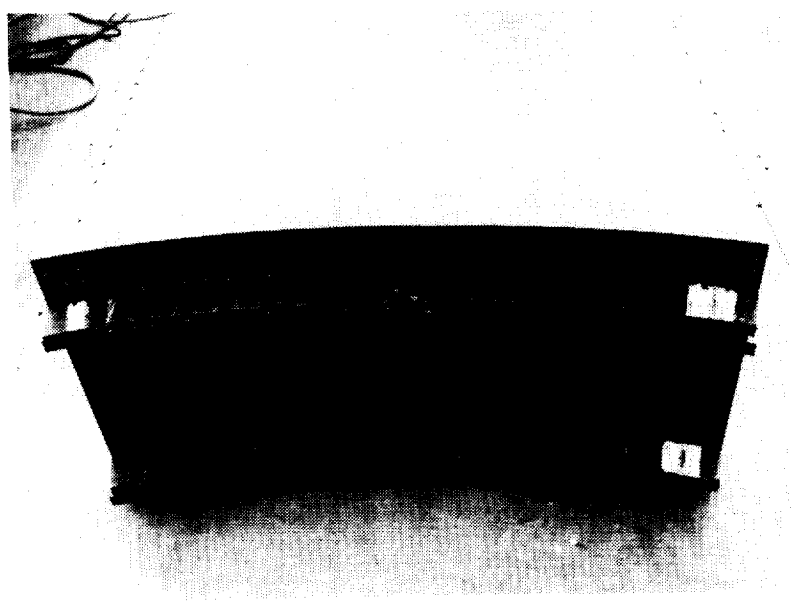

(b) Composite panel-post test.

Figure 12.- Behavior of composite fuselage panel under static loading.

ORIGINAL PAGE
BLACK AND WHITE PHOTOGRAPH

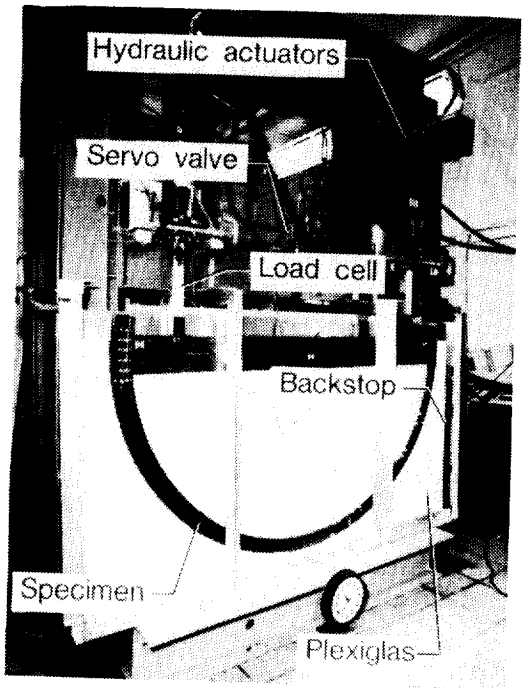

(a) Static test apparatus.

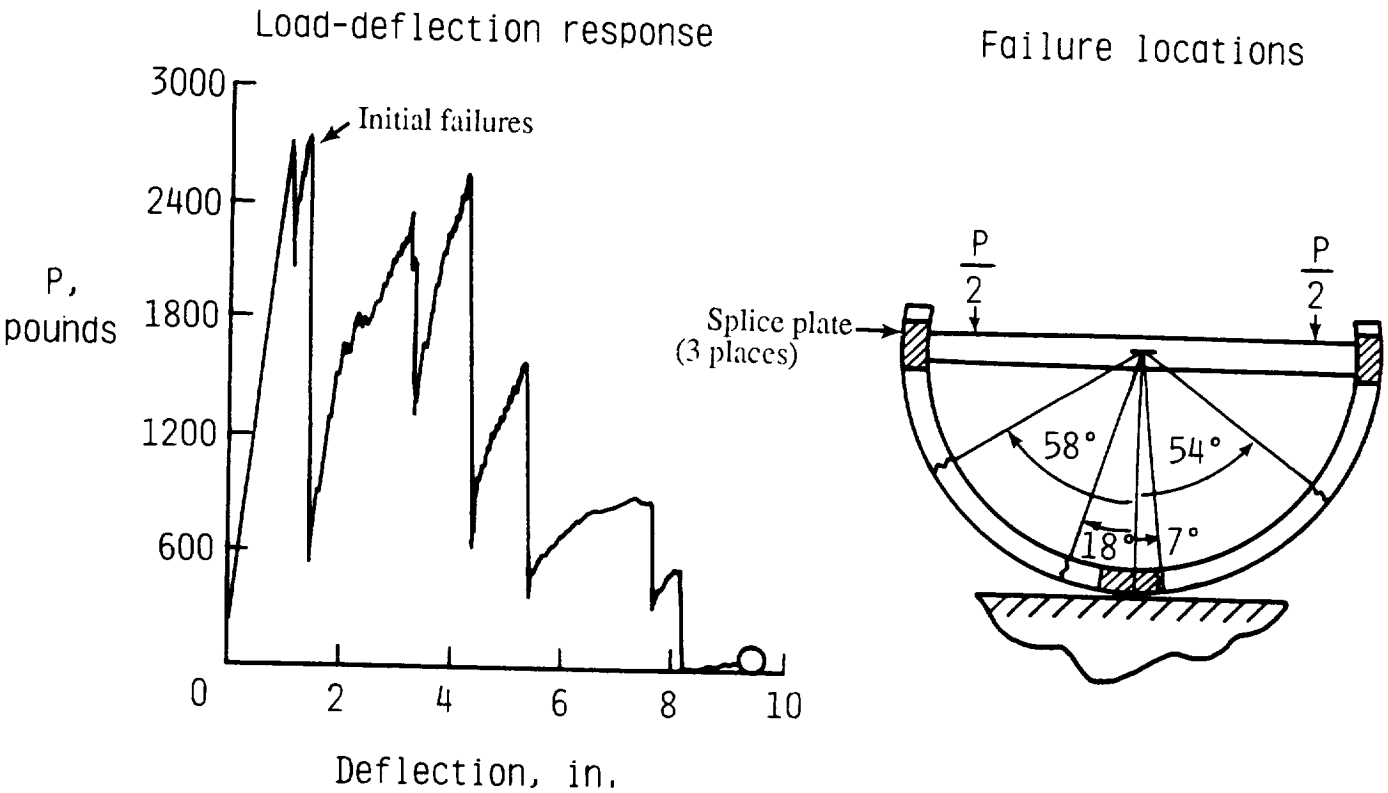

(b) Load-displacement and failure locations.

Figure 13.- Static results from tests of single composite Z-frame.

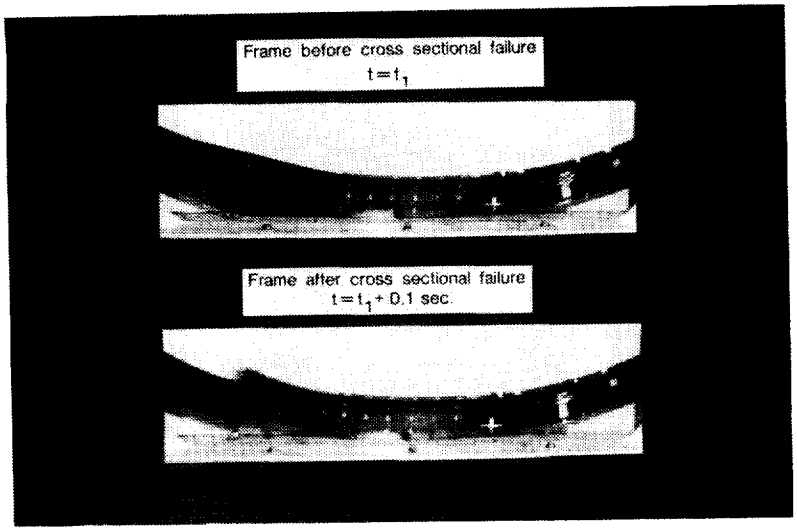

(c) Frame local instability.

Figure 13.- Concluded.

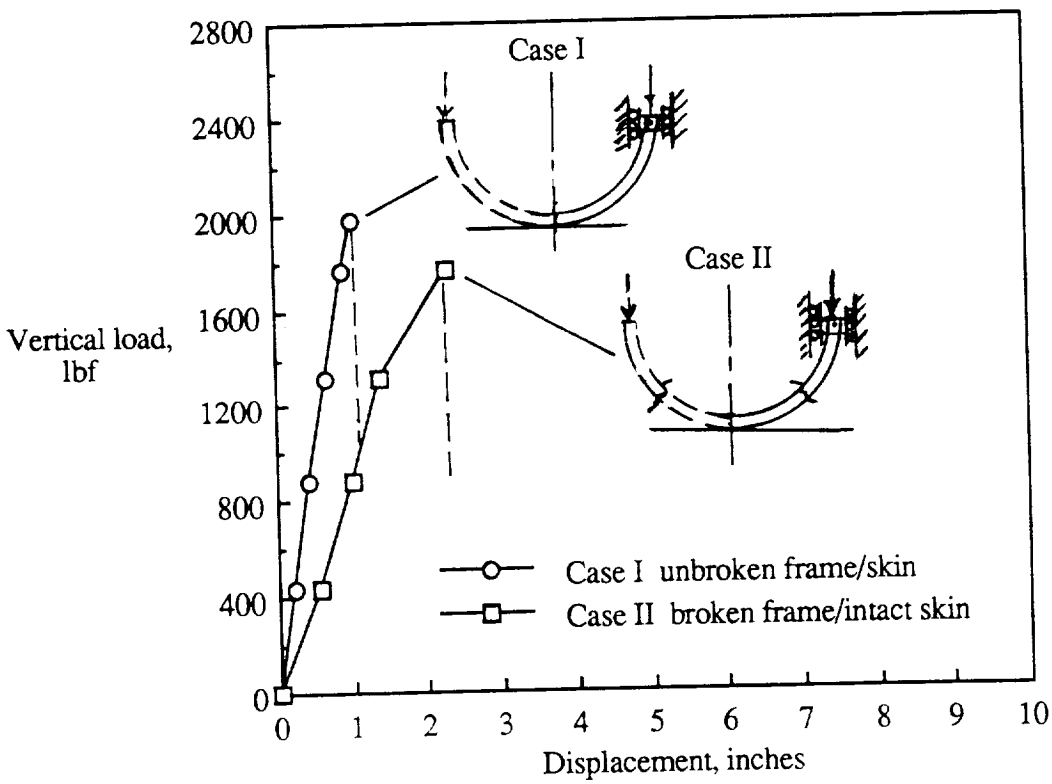

(a) Load-displacement.

Figure 14.- Typical analytical results for composite frame skin using I-section for ease of analysis.

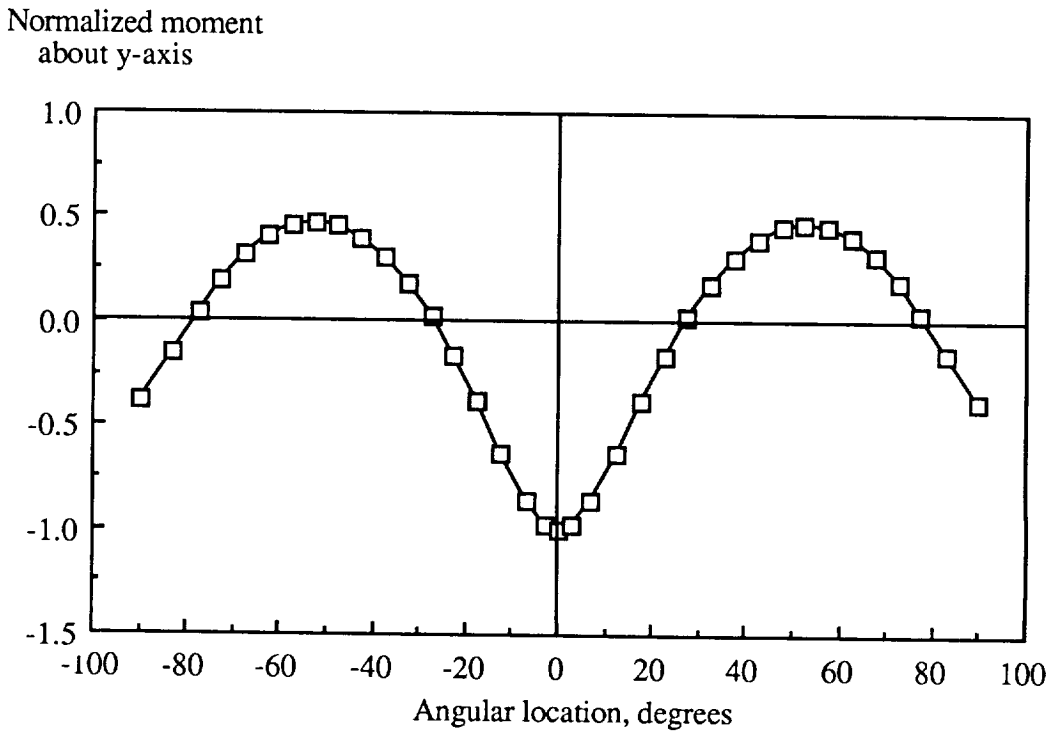

(b) Case I----Normalized moment (Prior to failure).

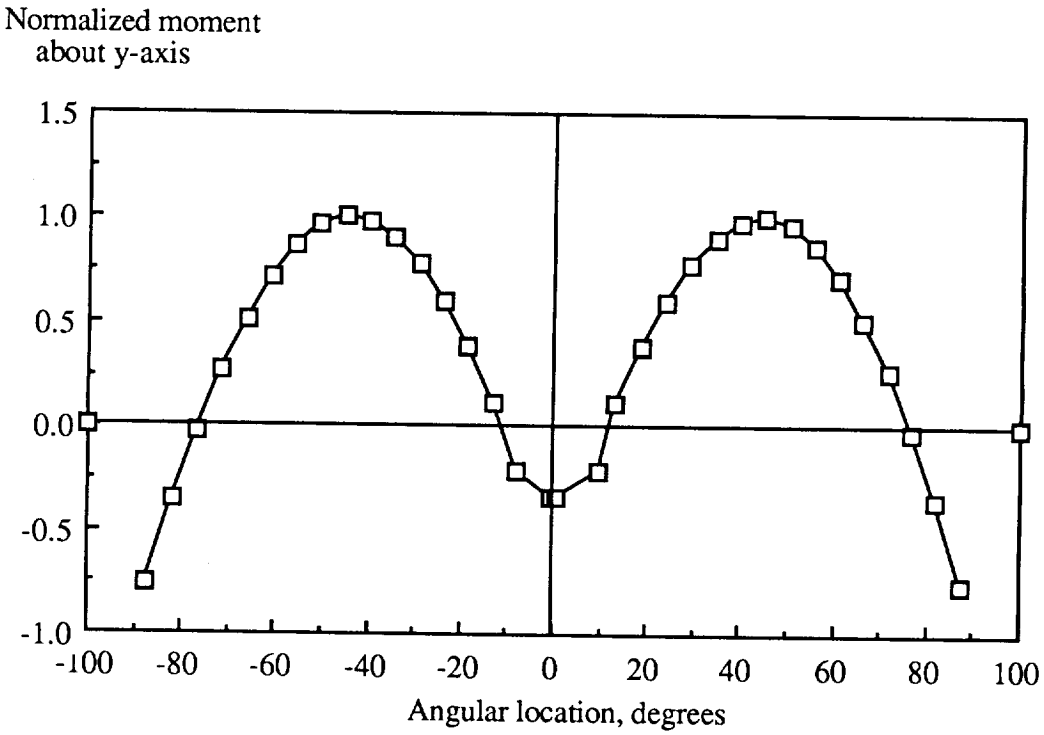

(c) Case II---Normalized moment (Broken frame-intact skin).

Figure 14.- Concluded.

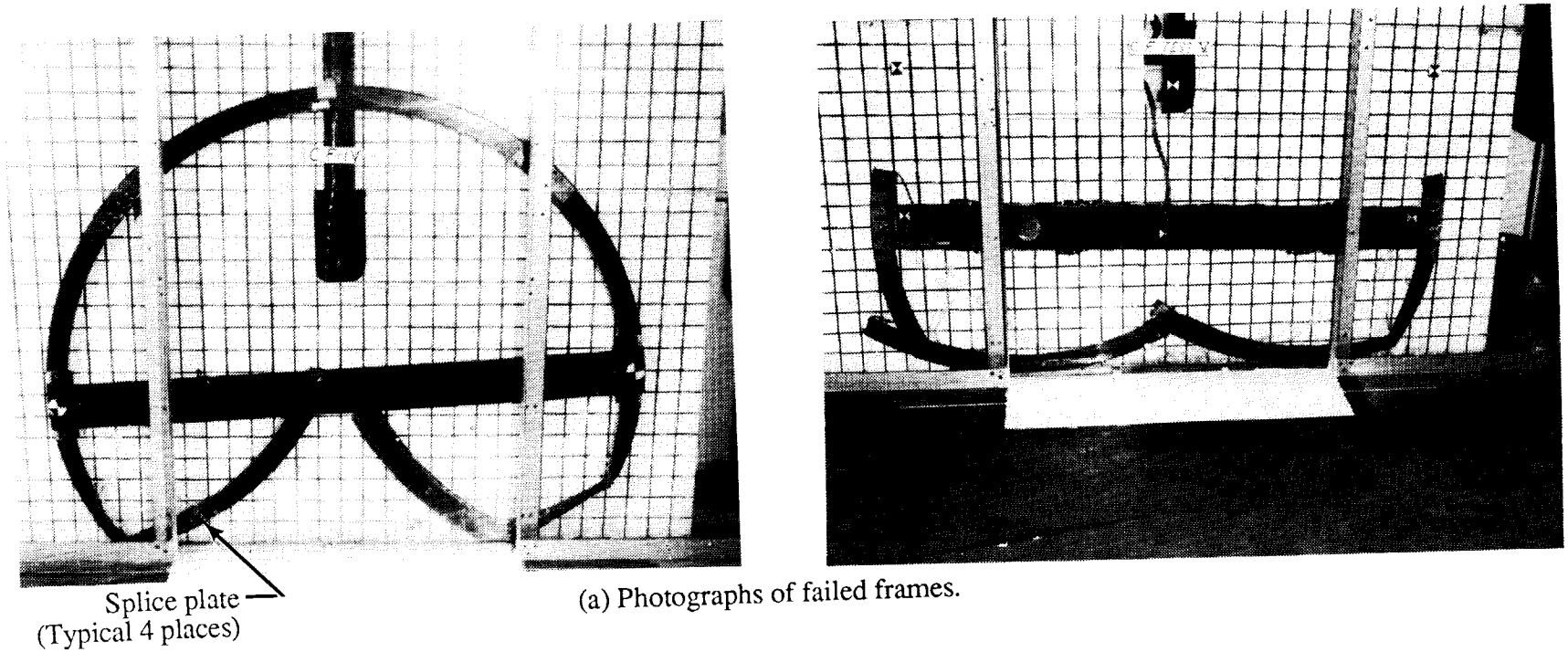

(a) Photographs of failed frames.

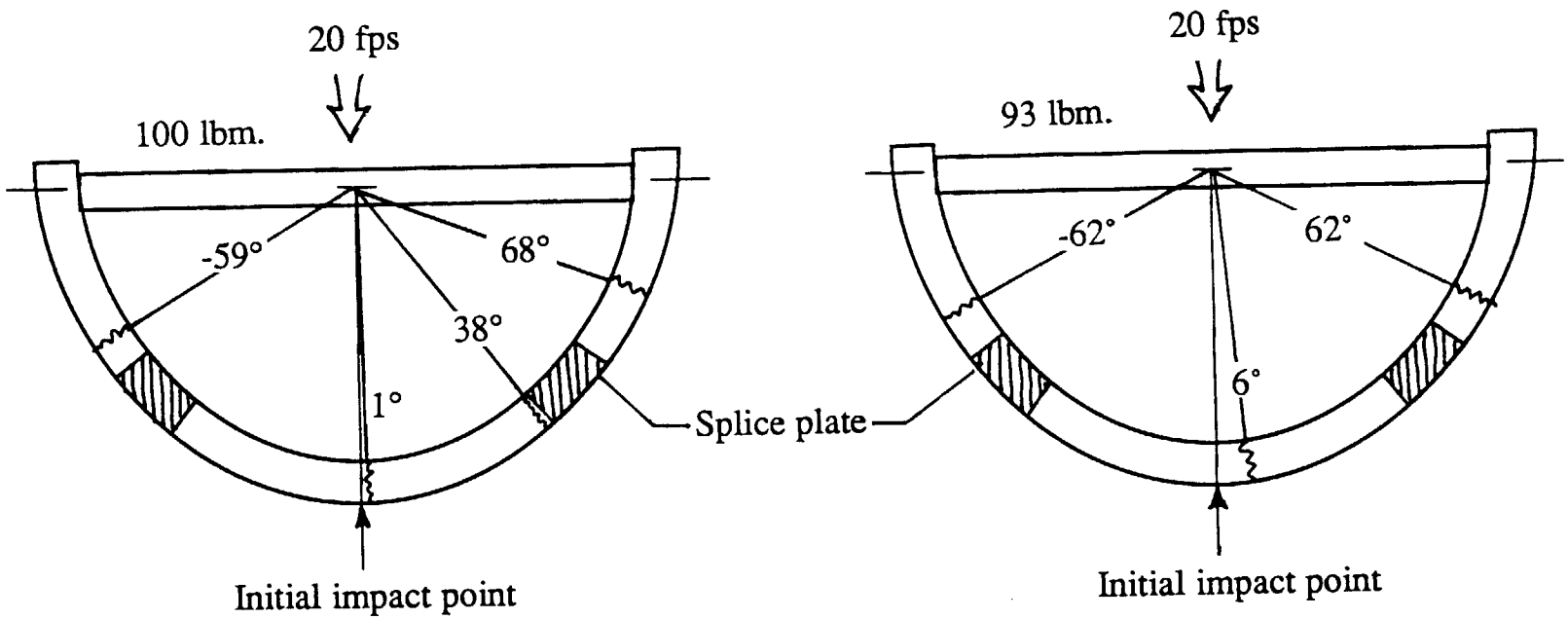

(b) Location of failures in frames.

Figure 15.- Behavior of composite Z-frame under dynamic loads.

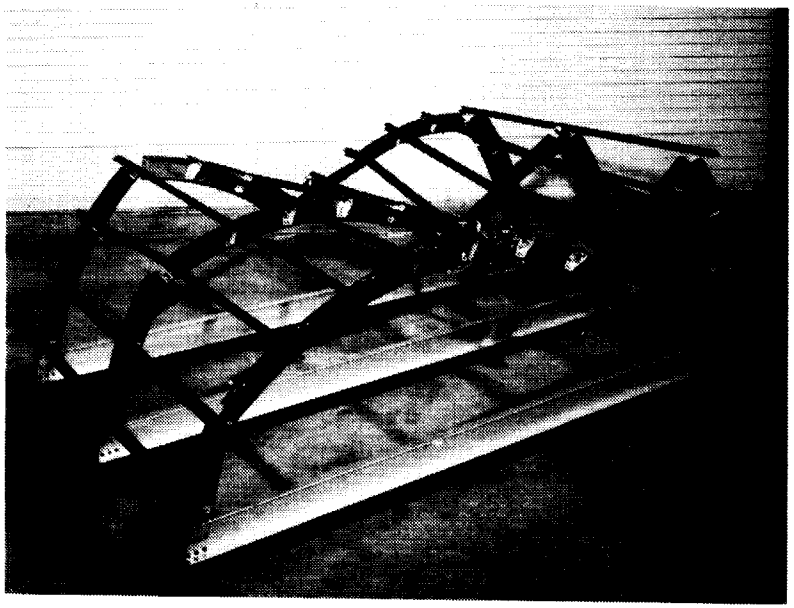

(a) Failed skeleton subfloor.

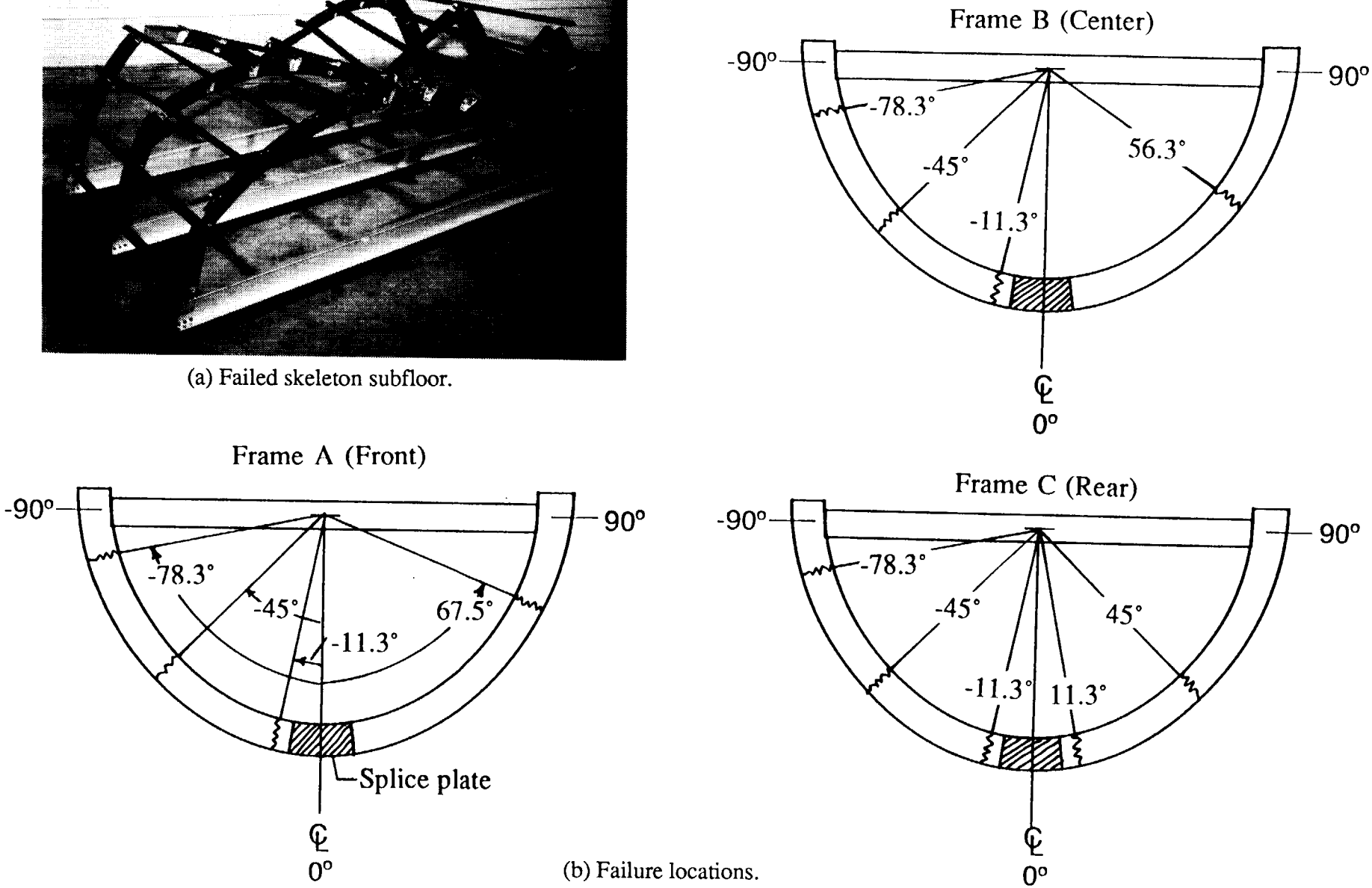

(b) Failure locations.

Figure 16.- Behavior of composite skeleton subfloor under static loading tests.

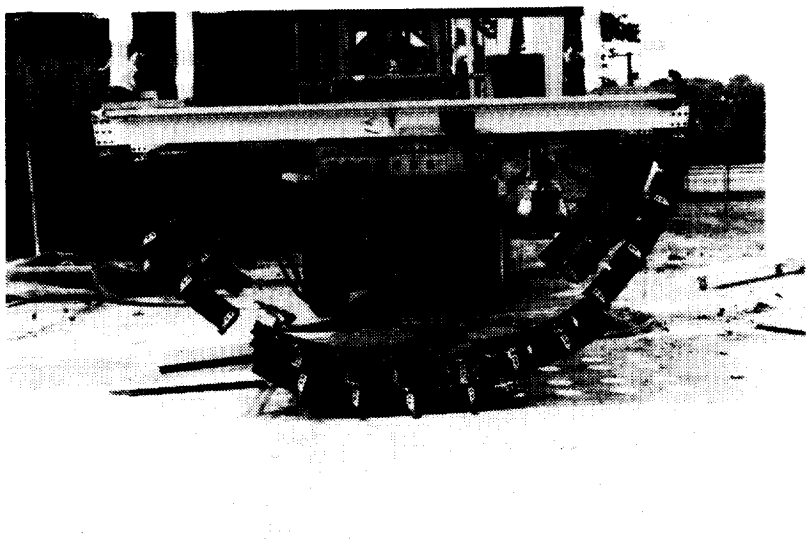

(a) Failed skeleton subfloor.

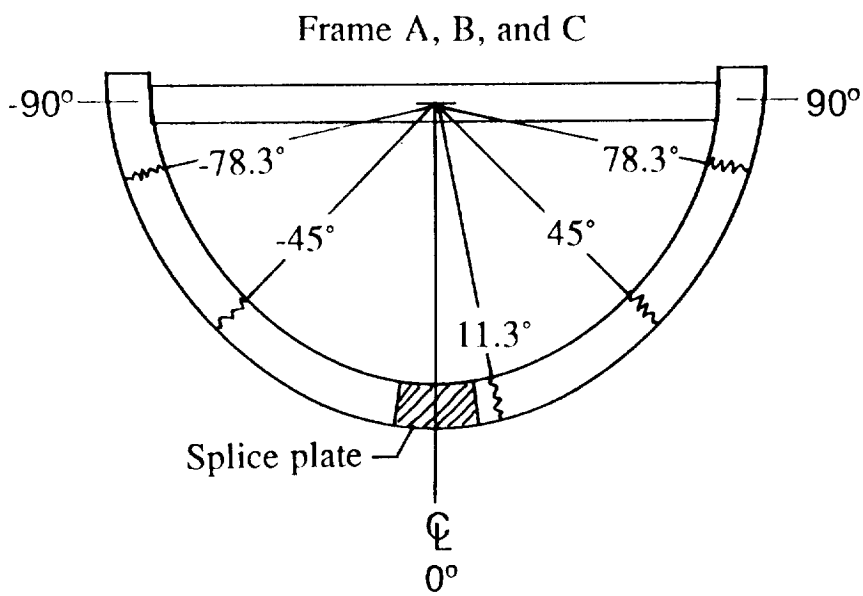

(b) Failure locations.

Figure 17.- Behavior of skeleton composite subfloor under dynamic loading tests.

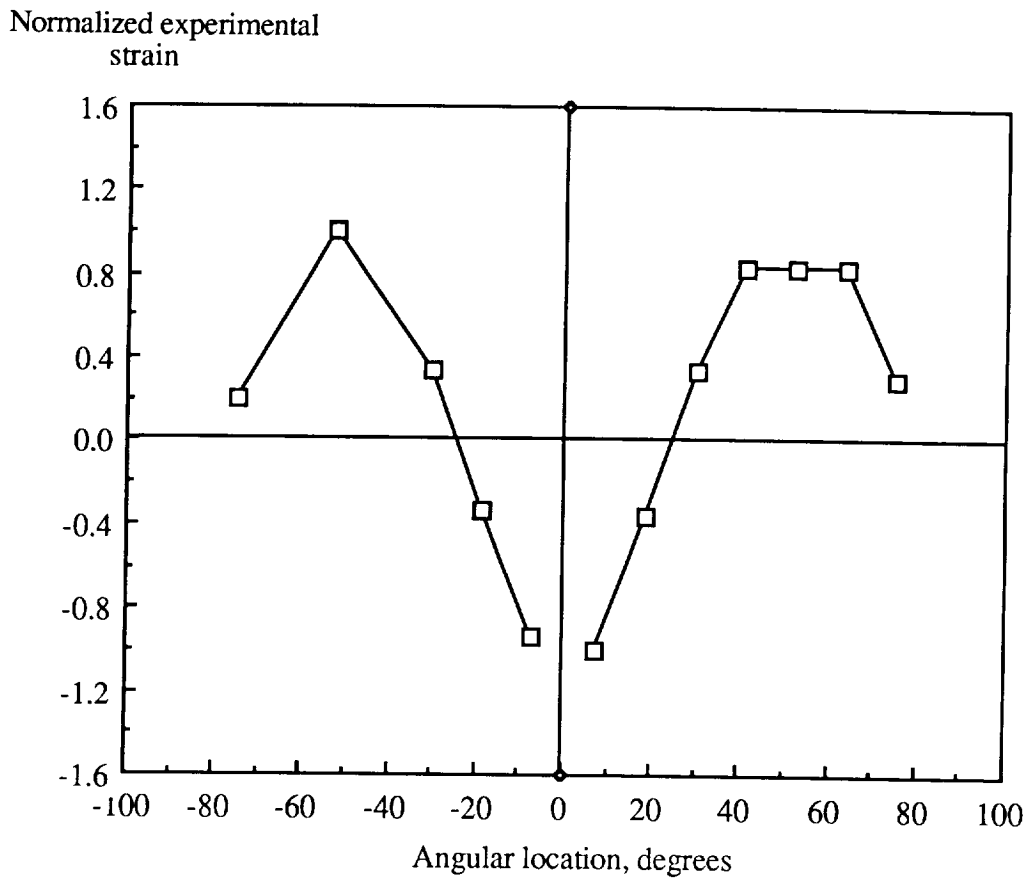

(c) Normalized strain distribution.

Figure 17.- Concluded.

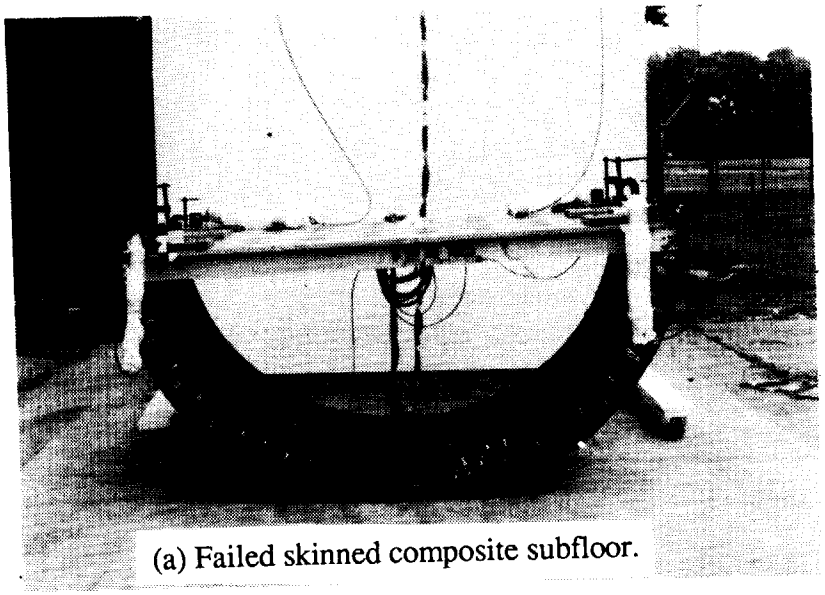

(a) Failed skinned composite subfloor.

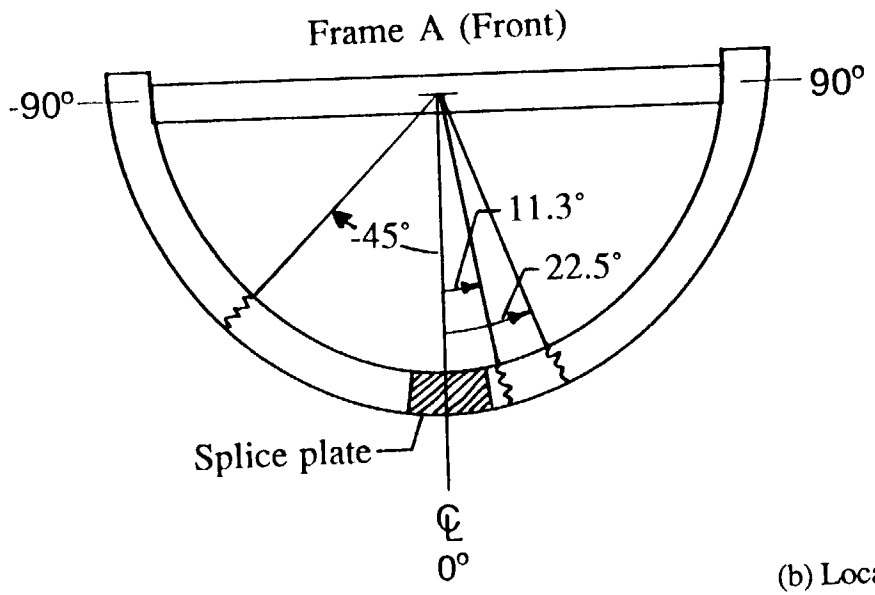

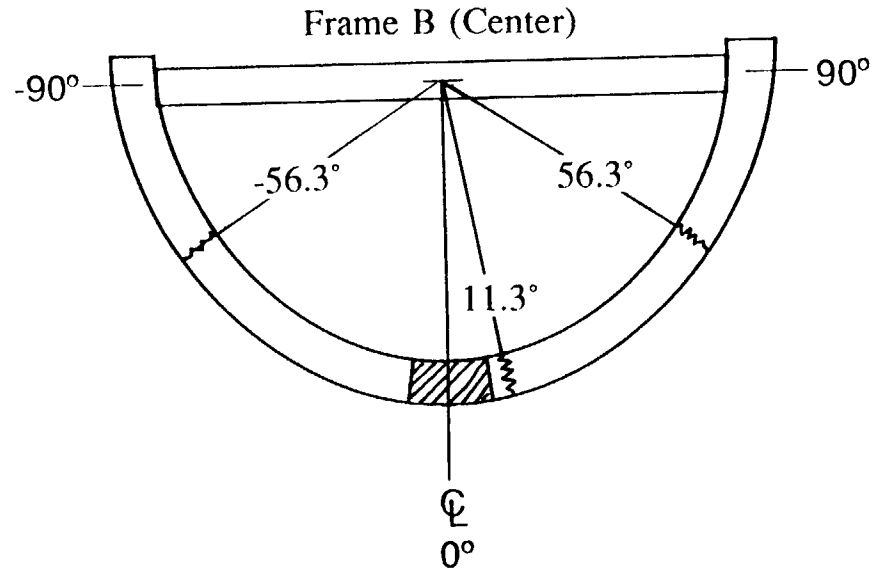

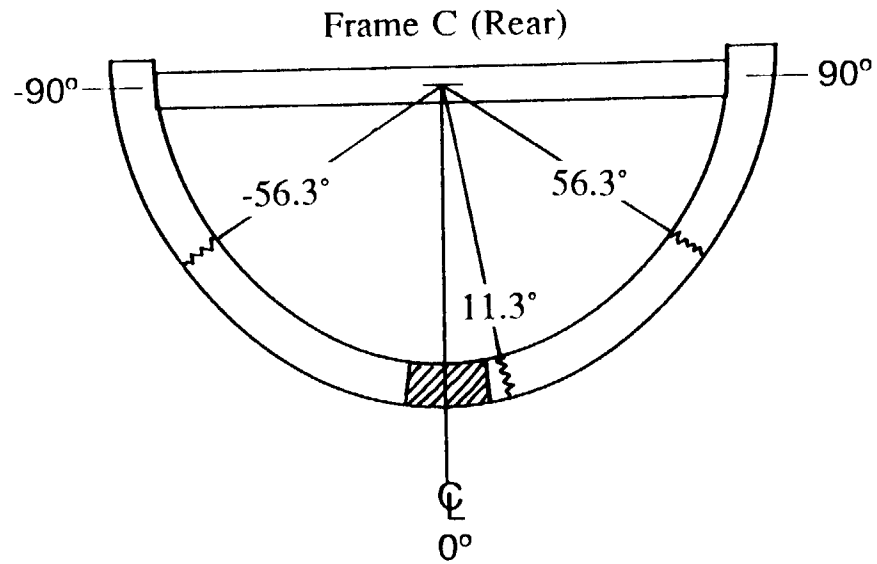

(b) Location of failures.

Figure 18.- Behavior of skinned composite subfloor under dynamic loading tests.

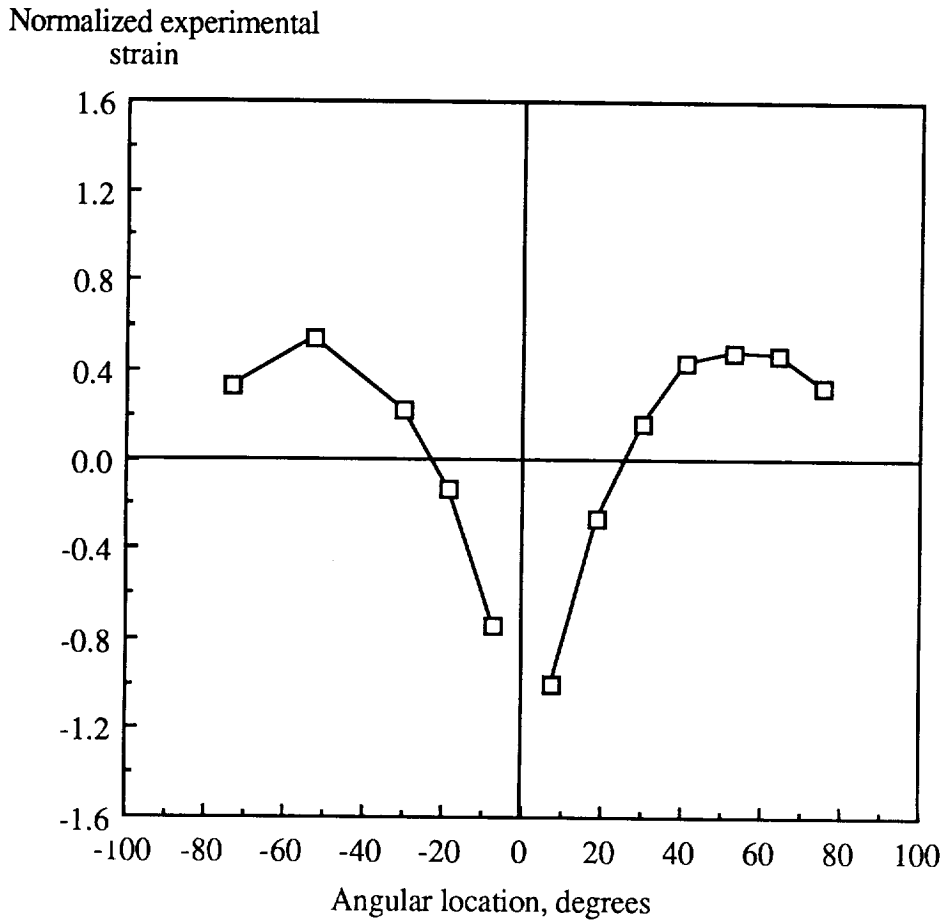

(c) Normalized strain distribution.

Figure 18.- Concluded.

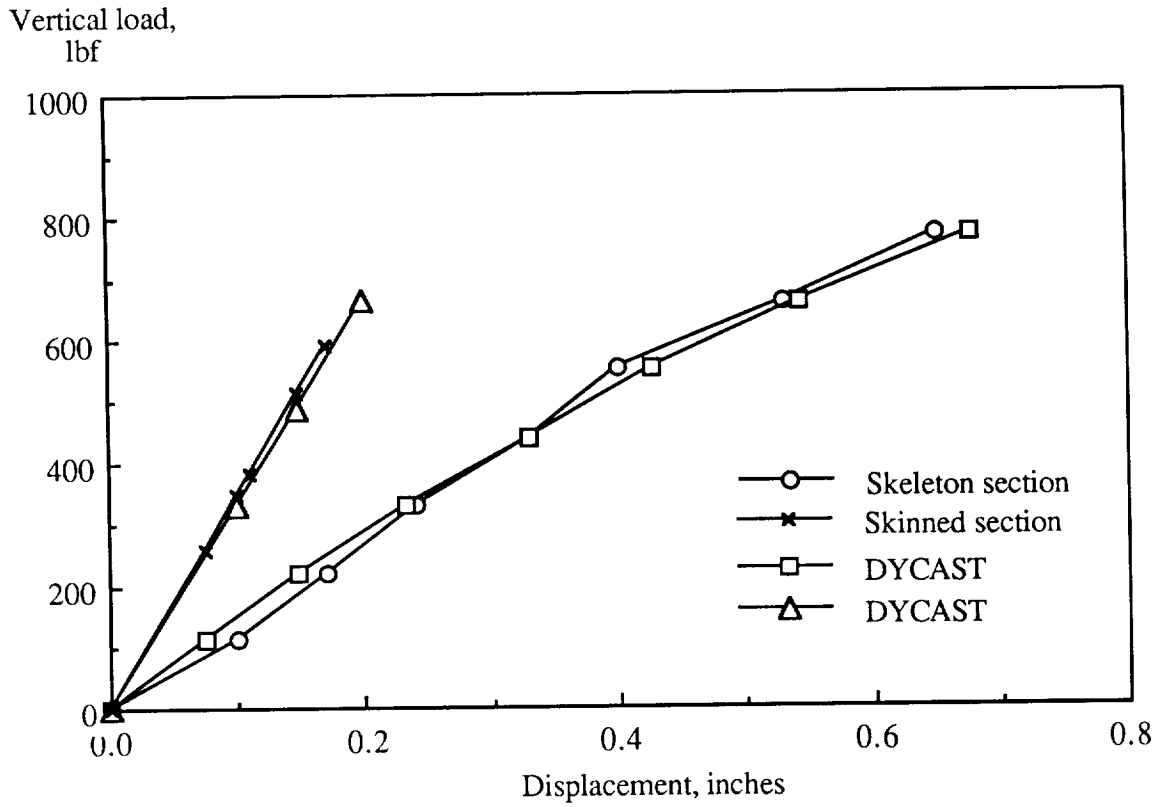

Figure 19.- Comparison of experimental and analytical stiffness of skeleton and skinned composite subfloors.

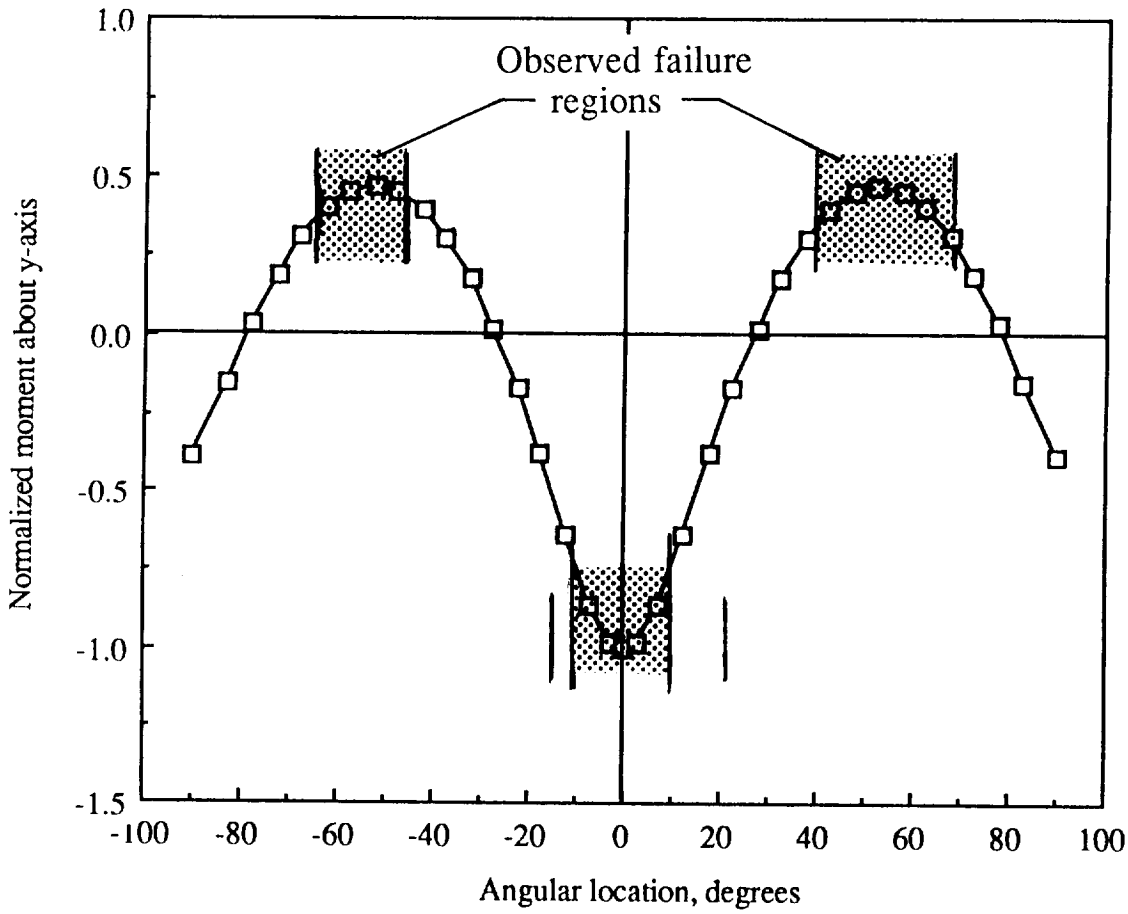

(a) Normalized moment distribution.

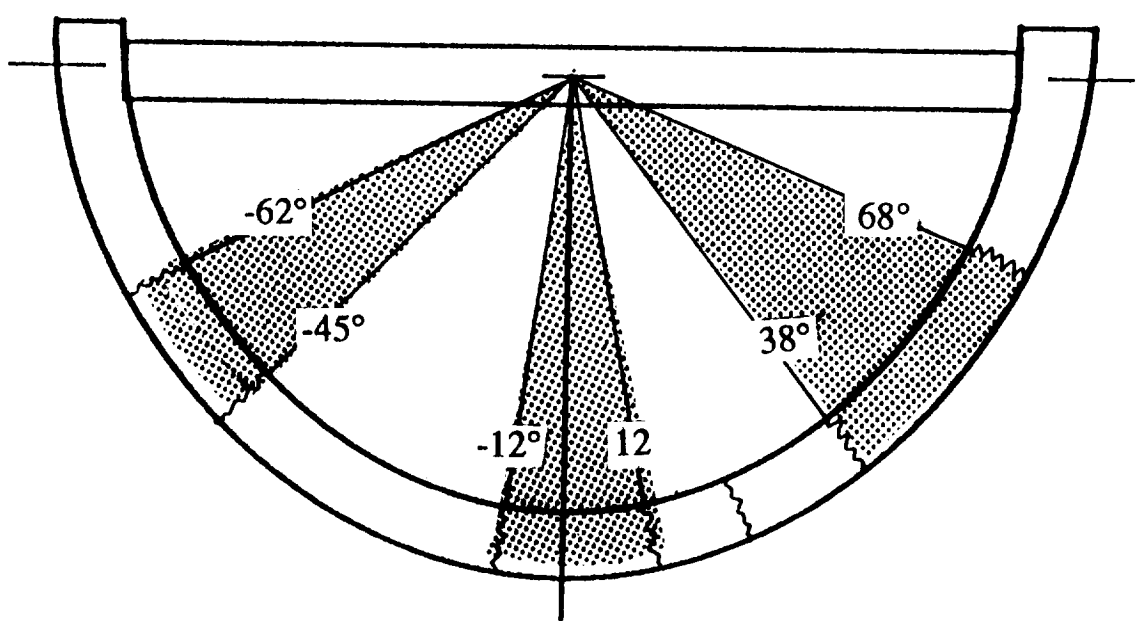

(b) Failure locations.

Figure 20.- Comparison of nondimensional analytical moment distribution predicted by finite element frame model and observed failure locations on metal and composite fuselage components and structures.